THE RADIATION AND GEOGRAPHIC EXPANSION OF EUPRIMATES THROUGH DIVERSE CLIMATES

Jorge Avaria-Llautureo [1]✉, Thomas A. Püschel[2], Andrew Meade[1], Joanna Baker[1], Samuel L. Nicholson[3], Chris Venditti[1]✉

1. School of Biological Sciences, University of Reading, UK
2. Institute of Human Sciences, School of Anthropology & Museum Ethnography, University of Oxford, UK
3. Climate Geochemistry, Max Planck Institute for Chemistry, Mainz, Germany

✉ Corresponding authors: j.l.avaria@reading.ac.uk; c.d.venditti@reading.ac.uk

Abstract

The most influential hypothesis about euprimate evolution postulates that their origin, radiation, and major dispersals, were associated with the exceptional warmer conditions of the planet in the tropical forests of higher latitudes. However, this notion has proven difficult to test given the overall uncertainty about the geographic locations and palaeoclimates of ancestral species. By the resolution of both challenges, we reveal that early euprimates dispersed and radiated in higher latitudes and through diverse climates defined by the Köppen-Geiger classification system, including cold, arid, and temperate. Contrary to expectations of the hypothesis, historical global temperature had no effect on dispersal distance or speciation rate. But how much the local temperature and precipitation changed substantially predicted geographic and species diversity. Our results set a new perspective on euprimate origins and evolution. They suggest that non-tropical and changeable environments exerted strong selective pressures on euprimates with higher dispersal ability which promoted this group's radiation and subsequent colonisation of tropical climates millions of years after their origin.

Introduction

The notion that early euprimates – all living primates and their ancestors [1] - originated, radiated, dispersed, and thrived in the tropical forests, has been the dominant narrative in the research about their origin, adaptation, and evolution, for more than four decades [2–17]. It is also often reported that their radiation dramatically expanded, both geographically and taxonomically, in association with the historical global warming of the Palaeocene-Eocene Thermal Maximum (PETM), when the range of the tropical forest presumably reached high latitudes into the Holarctic continents [5–7,14,18–21] (hereafter the tropical forest hypothesis). However, current evidence of palaeoclimate reconstructions based on the Köppen-Geiger (KG) climate classification system and simulations obtained from General Circulation Models (GCMs) - in regions exhibiting a higher density of early fossil euprimates - do not support the tropical climate expected under the tropical forest hypothesis. For instance, KG climate-reconstructions for the pre-PETM and PETM, based on both the spore-pollen fossils and the Community Earth System Model, Version 1.2 (CESM1.2), agree in that the KG-climates for important early euprimates locations, such as the Bighorn Basin and Chalk Butte (North America), were not tropical [22]. Also, several palynological fossil sites of the pre-PETM and PETM, across Western Europe, do not show evidence for tropical KG climates [22]. Additionally, independent simulations based on the Fast Ocean Atmosphere Model (FOAM) version 1.5, support the presence of non-tropical KG-climates across most of North America, Europe, and Asia, approximately 65 million years ago [23], which is where and when euprimates most likely originated [18,24–29]. Finally, Bayesian statistical analysis of lithologic, palaeontologic, and geochemical proxies does not support the presence of tropical KG climates across most of North America, Europe, and South Asia, close to the Early Cenozoic[30].

The mismatch between the euprimate tropical forest hypothesis and current evidence of palaeoclimates classified with the KG system, might be the result of several factors. First, there are inherent temporal, spatial, and taphonomic biases in the fossil record. These biases have made the tropical forest hypothesis a longstanding challenge to evaluate, mainly because the fossil record might be telling us more about the places, times, and climates where the fossilisation process is most likely. For example, it is recognised that the probability of fossilization is lower in tropical climates as compared to others [31]. Second, despite the tropical forest notion dominating the literature, there exists ambiguity about the specific concept and definition of the climate where euprimates originated and evolved. There are many names for the type of climate, including, continuous evergreen forest belt[7], tropical plants[14], lush forest[14], paratropical forest[5], and tropical angiosperm biome[15]. Therefore, to

overcome the enduring difficulty of evaluating the tropical forest hypothesis, it is essential to look at complementary evidence about the places where ancestral euprimates were thriving. It is also essential to use an explicit climate classification criterion to make the hypothesis testable, avoiding the ambiguity regarding the types of climates.

Here, we evaluated the tropical forest hypothesis (early euprimates originated, radiated, and moved longer distances, in the warmer global conditions of the tropical forest [2,3,5–7,10,14,16,18,32]) by first inferring the geographic locations of ancestral species in the phylogenetic tree. We reconstructed ancestral locations using a novel version of the Geographical (Geo) model in BayesTraits v4 [33,34] and the most complete phylogeny of extant and extinct (fossils) euprimates to date [28] (Methods). The Geo model provides a posterior distribution of longitude and latitudes for all internal nodes in a phylogenetic tree (i.e., pseudo-extinct species) [35], based on the geographic distribution of extant and fossil diversity as input data. The model samples the intraspecific variation in occurrence data for extant and fossil tips according to their probability. As the Geo model converts longitude and latitude data into coordinates in three-dimensional space (x, y, and z), the Geo model considers the spherical nature of Earth. This means that we were able to infer the geographic route and distance that each ancestral species travelled over the globe, allowing us to calculate and reconstruct the geographic pathway that each extant and extinct species took from the root of the phylogenetic tree (i.e., pathwise distance, $D_{PATHWISE}$; Methods).

Notably, the new Geo model allows map restrictions which enables us, for the first time, to account for the ancient distribution of the world's land and oceans while reconstructing ancestral locations. This new approach with palaeo-map restrictions is of fundamental importance when evaluating hypotheses about the historical biogeography and palaeoclimates of euprimates, as the dramatic ancient long-distance dispersal hypothesised to occur across Holarctic continents has long been linked to the relative position and connection/disconnection among continents in deep time [20,36].

Second, we extracted the monthly values of palaeotemperature and palaeoprecipitation from the ancestral species locations (Methods). For phylogenetic nodes, we extracted the palaeoclimate data from the posterior distribution of coordinates inferred with the Geo model with map restrictions. For fossils, we extracted the climate data from their palaeo coordinates (Methods). The palaeoclimate data of monthly precipitation and temperature was obtained from simulations based on the Hadley centre general circulation Coupled Model (the HadCM3BL-M2.1aD model, Methods) [37–39]. The performance of the HadCM3BL-M2.1aD in simulating modern climate is comparable to the current Coupled Model Intercomparison Project (CMIP) 5 and 6, state-of-the-art models [39,40]. General circulation models like the HadCM3BL-M2.1aD have been widely used in current palaeoclimate research that have brough meaningful inferences about palaeoclimate and diversity. Some examples include the FOAM and the CESM model [22,23,41–43].

Third, we formally classified the climate for every phylogenetic node and fossil based on the KG climate classification system [44,45]. The KG system classifies climates, based on monthly values of precipitation and temperatures, into the following main categories: Tropical (A), Arid (B), Temperate (C), Cold (D), and Polar (E). There are also several subcategories, e.g., Tropical Rainforest (Af), Tropical Monson (Am), and Tropical Savannah (Aw) (Methods). The KG classification reflects climatic factors limiting vegetation growth and has been widely applied to palaeoclimate simulations [22,23,41]. The KG system has several advantages over other climate classification systems in terms of applicability, comparability, and quantifiability [46]. The KG classifications allow us to make the euprimate tropical forest hypothesis explicitly testable, as the KG classification solves the difficulties related to inconsistent descriptions and semantic heterogeneity of climates definitions in the euprimate tropical forest hypothesis. As the ancestral locations at phylogenetic nodes are inferred based on the geographic distribution of extant and fossil diversity - not on their type of climates – while accounting for the non-independence in the geographic data, our approach allows us to reconstruct ancestral locations and climates that do not occur in the fossil or extant diversity. Finally, we extracted the historical global average temperature (*GT*), across every million years [47], to evaluate its expected positive effect on the euprimate radiation and geographic dispersal [5,7,18,48].

Our novel methodological approach brings the unique opportunity to test, for the first time, the longstanding tropical forest hypothesis that seeks to explain the geographic expansion and evolution of early euprimates. First, if ancestral species evolved and relied on the tropical forests for their dispersal, we would expect to find the climate reconstruction of all or most of the early phylogenetic nodes falling within the main KG climate category Tropical (A, Fig. 1a and b) [44]. The Tropical climate category refers to an environment that is hot all year round with average annual temperature over 18 °C [44,45]. This climate includes the subcategories Tropical Rainforest, Tropical Monsoon, and Tropical Savannah, which differ in the annual amount of rainfall[44,45]. Therefore, our prediction is conservative regarding the tropical forest hypothesis, as the Tropical climate considers

all the potential types of tropical climates where euprimates were proposed to originate and diversify. Second, if early euprimates dispersed greater distances during the warmest global conditions of the PETM – when the tropical rainforests reached their widest latitudinal extension [5,18,24] – we would expect to observe a negative association between $D_{PATHWISE}$ and time, i.e., there would be greater pathwise distances in the past, when the planet was exceptionally warmer (Fig. 1c). Third, we expect to observe a positive effect of *GT* on $D_{PATHWISE}$ (Fig. 1e, f). Fourth, if early euprimates were also more speciose during the PETM, we would expect to observe a negative association between pathwise node count ($NC_{PATHWISE}$) and time (Fig. 1d). $NC_{PATHWISE}$ can be regarded as a speciation rate metric obtained by counting the number of nodes between the root of the phylogenetic tree and every fossil and extant species [49]. Finally, we should observe a positive effect of *GT* on $NC_{PATHWISE}$ (Fig. 1g, h).

To test these predictions of the tropical forest hypothesis, we carried out phylogenetic generalized least squares (PGLS) models using $D_{PATHWISE}$ as the response variable, with time and *GT* as predictors. Then, we carried out phylogenetic generalized linear mixed models [50] (PGLMM) using the same predictors but using $NC_{PATHWISE}$ as response variable (Methods).

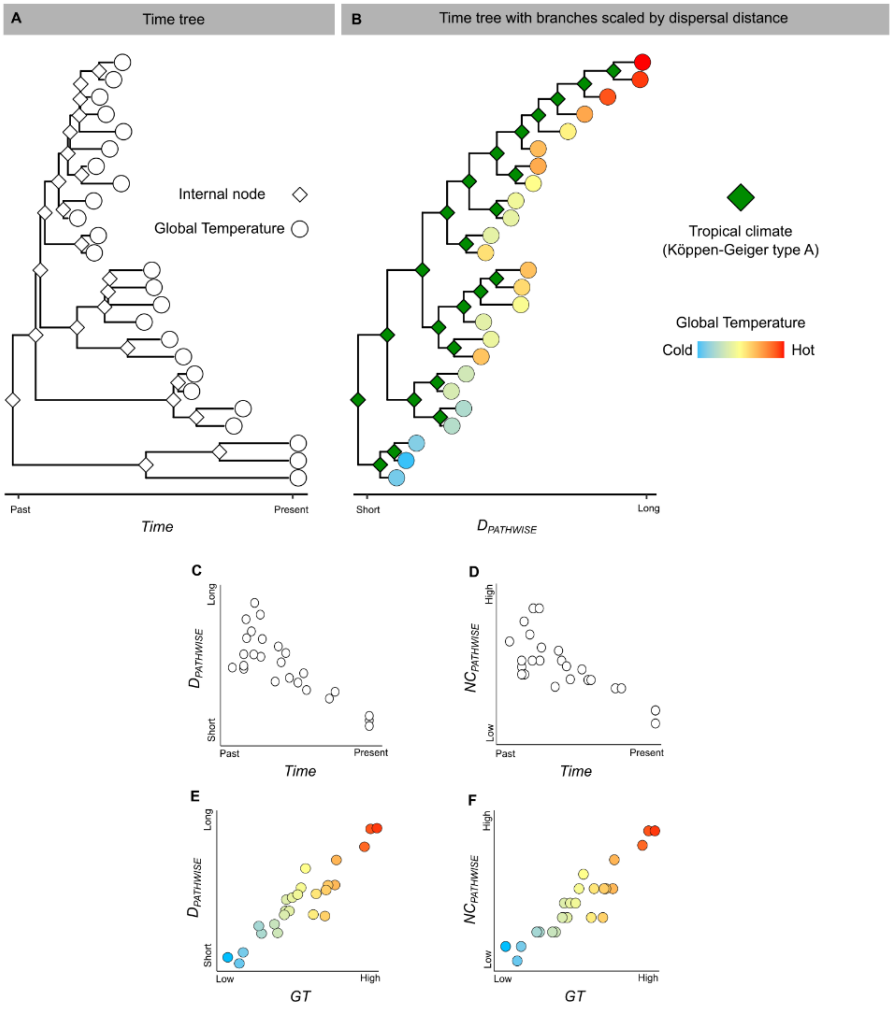

Figure 1. Expected results under the tropical forest hypothesis. **A.** Time-calibrated phylogenetic tree of fossils and extant species. White-filled diamonds are the internal nodes (ancestral species). White-filled circles represent the global temperature (GT) that each species was experiencing at a respective time. **B.** Time tree with branch lengths scaled according to the geographic distance each species dispersed. Green filled diamonds represent the Köppen-Geiger Tropical climate (A) for ancestral species. Circles filled with colour gradients represent the GT. **C.** The expected negative relationship between pathwise distance ($D_{PATHWISE}$) and time if early euprimates dispersed longer geographic distances. $D_{PATHWISE}$ is the sum of all the geographic distances across the branches that link the root of the tree with every phylogenetic tip. Time is the sum of all the branches that link the root of the time tree with every phylogenetic tip. **D.** The expected negative relationship between pathwise node count ($NC_{PATHWISE}$) and time if early euprimates speciated at higher rates. $NC_{PATHWISE}$ is the number of nodes, or speciation events, between the root of the tree and every tip. **E.** The expected positive relationship between $D_{PATHWISE}$ and GT if species dispersed longer distances during past warmer global conditions. **F.** The expected positive relationship between $NC_{PATHWISE}$ and GT if early euprimates speciated at higher rates during the past warmer global conditions.

Results and Discussion

Crown euprimate ancestral location and palaeoclimate. When we ran the Geo analyses using a single median phylogenetic tree (Methods) and world-maps to restrict the locations for all internal nodes, the geographic distribution of the crown euprimates most recent common ancestor was inferred across North America in 8 of 10 analyses. In the other two Geo analyses, we found Western Europe as the most likely location. When we ran the analyses on a sample of 100 phylogenetic trees, which includes both topological and temporal uncertainty (Methods), we found North America as the location for the common ancestor in 70% of trees, and Western Europe in the other 30% of trees (Extended Data Table 2). Those two likely locations are expected if we consider the location of some of the oldest fossil euprimates like *Teilhardina magnoliana* and *T. brandti* in North America [18,51], and *T. belgica* in Western Europe [52].

However, as euprimates first appear in the fossil record of Asia, Europe, and North America, almost synchronously [7,18], and given that some previous research has suggested that the location could also be Africa [26], we explicitly compared the model fit of these four potential locations (Fig. 2a, b). To do this, we additionally used four continental-map restrictions to restrict the location for the common ancestor to be inferred only in Africa, Asia, Europe, or North America (Fig. 2a), and we ran 10 Geo analyses for each model. Comparison of these Geo models, based on their marginal likelihoods estimated by stepping-stone sampling[53] (Methods), showed that the model with the common ancestor restricted to be in North America fit the data best (Bayes Factor > 5; strong evidence; Fig. 2b), which agrees with previous findings [25,51]. Finally, when we ran the Geo model analysis on 200 input data sets where we down sampled the fossils from northern latitudes (to mitigate sampling bias owing to taphonomic issues determining a higher density of early fossils in northern latitudes) we obtained North America as the most likely location for the common ancestor in 80% of the 200 data sets (Supplementary Data S11).

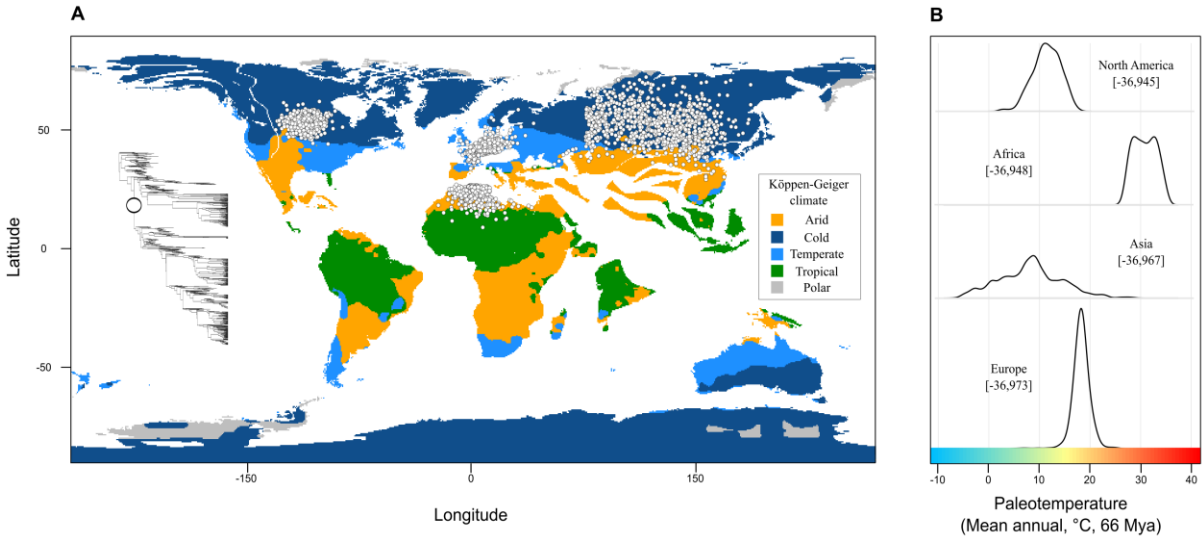

Figure 2. The location of the common ancestor of the crown Euprimate was North America. **A.** world palaeo map with the Köppen-Geiger main climates of 66 million years ago. White circles on the map are the posterior distribution of coordinates for the common ancestor (white circle on the tree). These coordinates were inferred using the Geo model with map restrictions. We ran four Geo models, restricting the location to be either in North America, Africa, Asia, or Europe. **B.** mean annual palaeotemperature extracted from the posterior distribution of coordinates across each continental location. The continental locations are ordered by their marginal likelihood inferred by steppingstones (numbers in squared brackets), with the best fit model on top.

The geographical location is of critical importance if we are to make inferences about the physiological nature of the common ancestor. This is because the mean temperature across North America, Africa, Asia, and Europe, 66 million years ago, varied from ~8 to ~30 ºC (Fig. 1b); and it is well known that temperature plays a crucial role in determining the physiological nature of endothermic organisms like primates [54]. Furthermore, the monthly palaeo temperature extracted from the posterior distribution of coordinates for the common ancestor in North America, indicates a cold (type D) KG climate (Fig. 2a, Supplementary Data S12). This particular result implies that euprimates transitioned to tropical climates after their origin.

Historical climatic transition. Our climate reconstructions across phylogenetic nodes reveal that the dominant climate that ancestral species inhabited changed dramatically through time (Fig. 3a, b). This is contrary to the general notion that they mostly relied on tropical climates [5]. Rather, we show that most early euprimates

occupied cold, temperate, and dry climates (Fig. 3a, b). This result does not support the first expectation of the tropical forest hypothesis, i.e., a climate reconstruction of all or most of the early phylogenetic internal nodes falling within the main KG climate category Tropical (Fig. 1A). Our climatic reconstruction pattern stands over the sample of 100 phylogenetic trees (Supplementary Data S7), which means that our results are robust to the topological and temporal uncertainty in the phylogenetic tree, and to the uncertainty of ancestral locations inferred with the Geo model across the sample of trees (Extended Data Table 2).

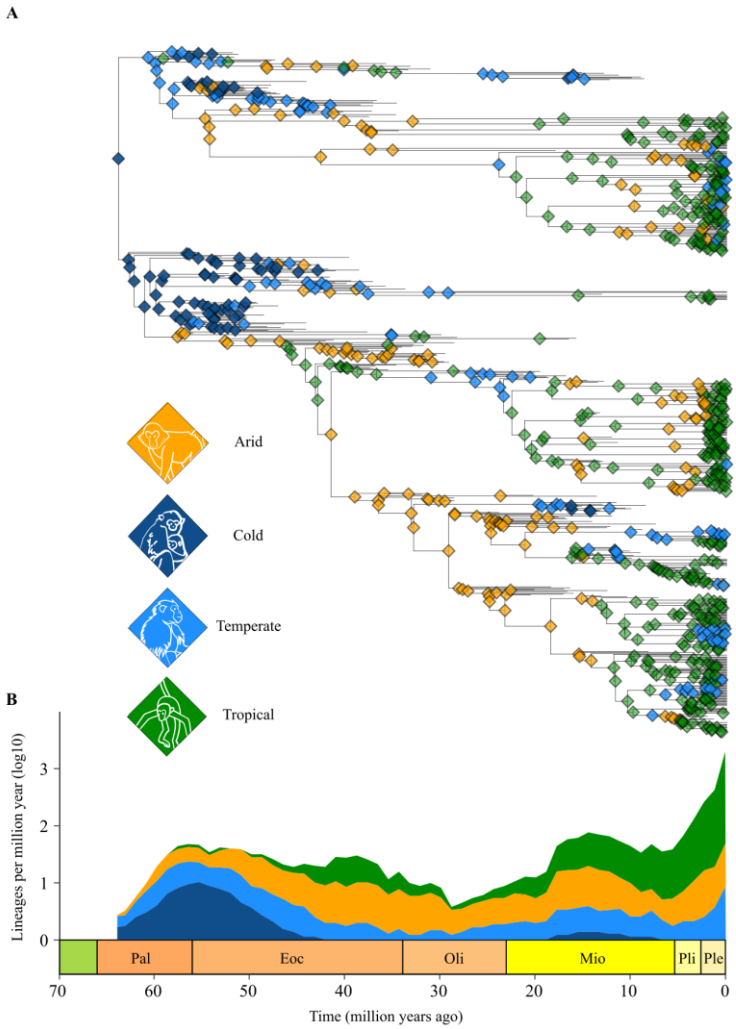

Figure 3. Ancestral euprimates inhabited diverse climates. **A.** Euprimate median phylogenetic tree with the Köppen-Geiger main climates categories for all internal nodes. The climate reconstruction was obtained by extracting the monthly palaeotemperature and precipitation (simulated under the HadCM3BL-M2.1aD climate model) from the Geo model posterior node coordinates. **B.** lineages through time intervals of one million years. Fossils and extant species are also included in this plot. Colours represent the proportion of lineages inhabiting each climate category through time.

Additionally, our ancestral climatic reconstruction remains qualitatively similar even when we ran all the analyses on the 200 input data sets that are heavily biased against non-tropical fossils in northern latitudes (Methods, Data 10 and 11). If the taphonomic bias favouring fossilization in non-tropical climates was influencing our node climates to be reconstructed as non-tropical, then we should observe an increase of tropical climates across phylogenetic nodes when running the analyses on input data that randomly down sample the non-tropical fossils; but this expectation was not supported by the evidence (Supplementary Data S11).

When looking at the change in climate along branches (i.e., between the main of the KG climates categories; arid, cold, temperate, and tropical, Fig. 3a) we see that climate transitions are relatively rare. Specifically, 22% of phylogenetic branches showed transitions in the main KG climate between ancestral and descendant nodes. However, when examining the ancestor-descendant KG climate subcategories (Supplementary Table 12), we can see that the sub-climatic transitions are relatively more common (39% of branches). On the other hand, of the ~22% of branches that showed transitions between main KG climates, the most common one

was from arid to tropical (~5% of branches), followed by tropical to temperate (4% of branches) (Fig. 4a). The least frequent transitions were from tropical to cold, and from cold to tropical (< 1 % of branches; Fig. 4a). Transitions from cold to any other climates were also rarely observed (< 2 % of branches; Fig. 4a). These branches showing main climatic transition were associated to longer geographic movements (median distance transitional branches = 561 km; median distance non-transitional branches = 137 km), which means that the major historical colonisations of novel main KG climates were linked to long distance dispersals. Taken together, our results demonstrate that euprimates have had the ability to disperse and colonise diverse KG climate subcategories, where those longer dispersal distances were associated to major main KG climatic transitions.

To delve further into the historical transition between main KG climate categories and to provide a comprehensive understanding of its temporal pattern, we elaborate on the transitions across three temporal windows, namely, from 66 to 47.8 Mya (early), 47.8 to 23.03 (middle), and 23.03 to the present (late; Fig. 4b, c, and d). Those temporal windows reveal that most of the transitions in early euprimates radiation were from the cold to the temperate climate (Fig.4b). In middle of the radiation, most of the transitions occurred from the temperate to the arid climate (Fig. 4c). During the late radiation, major transitions occurred from the arid to the tropical climate (Fig. 4d). This late radiation pattern seemingly coeval to the global trend to drier and cooler climates of the Neogene (since 23.03 Mya), and the expansion of the major mid-latitude deserts (e.g., Saharo-Arabia). During the Neogene, the Earth cooled down and experienced the onset of ice sheet expansion and expansion of the Mid-Latitude deserts. Perhaps such climatic changes may have caused the dispersals and transitions into tropical climates [55–57].

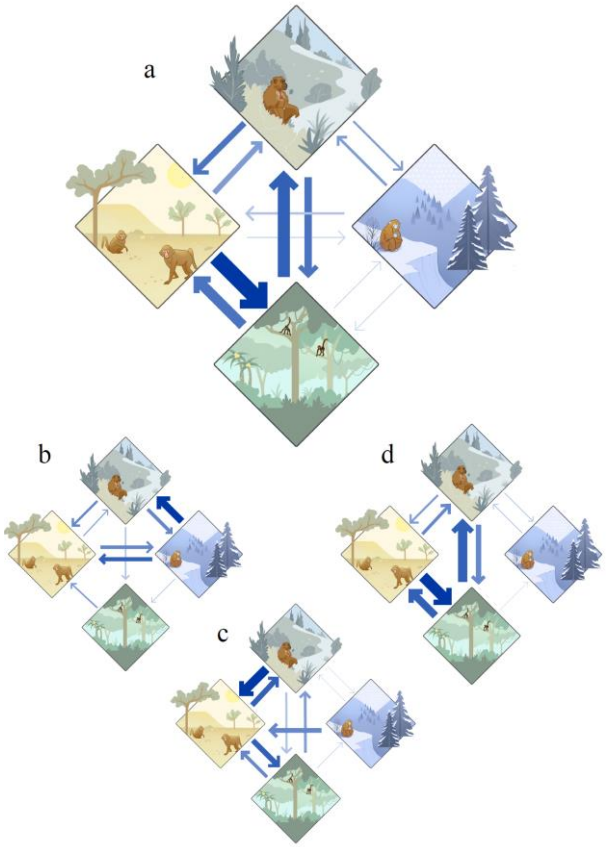

Figure 4. Euprimates historically transitioned across the Arid, Temperate, Tropical, and Cold Koppen-Geiger climate categories. (A) Transition between the Temperate (top), Arid (left), Tropical (bottom), and Cold (right), main climates, for all euprimates. Arrow size represents the proportion of phylogenetic branches with the respective transitions. (B) climatic transitions for early euprimates, who were living between 65 and 47.8 million years ago. (C) climatic transitions for species that were living between 47.8 and 23.03 million years ago. (D) climatic transitions for species that were living from 23.03 million years ago to the present.

Taken together, our results suggest that – contrary to what has been thought for more than four decades [2,5] – early euprimates were moving through, evolving in, speciating in, going extinct in, as well as mostly living

in the non-tropical climates of the northern continents. Our results also reveal a more complex evolutionary process in which euprimates were dispersing towards warmer climates in their evolutionary history, from cold, transitioning through temperate and arid, to finally disperse and colonise mostly the tropical climate.

As our conclusions are based partially on palaeoclimate simulations using GCMs which have associated error and error may bias our main findings, we additionally reconstructed ancestral climates by means of a different approach. We used only the observed KG climates for extant species and fossils species in the phylogeny and we reconstructed climates at internal nodes using a continuous time Markov model for discrete trait evolution[58]. We conducted this analysis on the single median tree and each of the100 trees. Using this alternative approach, we obtained qualitatively identical results for the ancestral climates (see Extended Data Figure 3).

The result showing that the most recent common ancestor was living in non-tropical climates has also significant implications for the study of euprimate origins. This is because some of the main hypotheses proposed to explain euprimate origin, such as the visual predation [2] and the terminal branch feeding hypotheses [4], postulates that the cognitive, locomotor, and life-history characteristic that define euprimates evolved under the stable, non-seasonal humid and warm conditions of the tropical forest. Despite that developing a new hypothesis for euprimate origins is not within the scope of our study, we think that the hypothesis proposed by[15] provides a valuable starting point. Those authors suggest that *"the dietary specialization - whether for visual predation or for angiosperm products - may not have been the primary force driving early primate adaptations. Instead, the evolutionary changes in angiosperms and forest structure, along with niche partitioning among diversifying Euarchonta, could have led ancestral primates to adapt to locomotion and foraging in the evolving angiosperm canopies"*. We add to that hypothesis the idea that the evolutionary changes in forest structure, along with niche partitioning, *in non-tropical forest*, could have led ancestral primates to adapt to locomotion and foraging in the evolving *non-tropical trees.*

Global temperature is decoupled from biogeographic movement and speciation. Even though early species did not live and expand mostly in the tropical forest, we might still identify the expected positive effect of global average temperature (*GT*) on speciation rate and dispersal distance. This would be true if the past hyper-thermal conditions of the globe - regardless of the type of climate - promoted their speciation and geographic expansion [5,7,14,18].

When we formally evaluated the effect of *GT* on $D_{PATHWISE}$ and $NC_{PATHWISE}$, we did not find a significant effect on any of the two response variables (Extended Data Table 3). Time had a significant positive effect on both $D_{PATHWISE}$ and $NC_{PATHWISE}$ (Extended Data Table 3), meaning that species dispersal distance and speciation rate were higher in the present rather than in the past. This result is expected by virtue that euprimates have had more time to move and speciate. Therefore, these results do not support the tropical rainforest hypothesis expectation, i.e., that the past warmer global temperatures, including those of the PETM, were associated to the highest species dispersal distances and speciation rates.

GT may not explain euprimates biogeographic movement and speciation because of the natural mismatch between global and local environmental conditions. Thus, perhaps local environmental conditions like local temperature (*LT*) and local precipitation (*LP*) where each species lives or lived might relate positively to $D_{PATHWISE}$ and $NC_{PATHWISE}$. To assess this expectation, we tested *LT* and *LP* in our phylogenetic regression models. Such local variables were obtained from palaeo coordinates for fossils, and from current coordinates for extant species (Methods). Our results show that *LT* had a significant effect on both response variables (positive on $D_{PATHWISE}$, negative on $NC_{PATHWISE}$; Extended Data Table 3). *LP*, on the other hand, had a significant negative effect on $NC_{PATHWISE}$ only (Extended Data Table 3). However, *LT* and *LP* explained less than 3% of the variance in $D_{PATHWISE}$ and $NC_{PATHWISE}$ (Extended Data Table 4). This means that there still exists wide uncertainty about what were the main factors that drove the dispersal and speciation of euprimates across multiple continents.

The rate of change in *LT* and *LP* substantially explains biogeographic movement and speciation. It has been proposed that the rate of climate change could be a factor of paramount importance in determining the geographic and evolutionary dynamic of euprimates [19,60–64]. In fact, during the PETM, *GT* not only increased to one of their highest records but also those historical increases were exceptionally fast [47,57]. Also, our results show that ancestral species dispersed and transitioned across diverse KG climatic subcategories (Supplementary Data 12), which differs substantially in the annual pattern of both *LT* and *LP* [44,45]. Examining the local climate variables allows us to explicitly test if changeable environment in a species history influenced $D_{PATHWISE}$ and $NC_{PATHWISE}$. Therefore, we tested the effect of the rate of local climate change on species dispersal and speciation by including the pathwise rate of local temperature (LT_{RATE}) and the pathwise rate of local precipitation (LP_{RATE}) to our phylogenetic regressions. The LT_{RATE} and LP_{RATE} is the cumulative change of *LT* and *LP* across the phylogenetic

branches that link the common ancestor with every fossil and extant species, divided by time (Methods; though the effect of these variables is identical when we do not divide by time). Crucially, these changes are not directional, i.e., changes can be to either cooler, warmer, drier, or wetter local conditions. These variables give us an estimation of the rate of change in *LT* and *LP*. It is the rate of local changes that each species experienced since the origin of the common ancestor, until the present for extant species, and, until the time each species went extinct in the case of fossils species.

We found that the LT_{RATE} and LP_{RATE} explained 19% and 2% of the variance in $D_{PATHWISE}$, respectively (Extended Data Table 4). Both rates of local changes related positively to $D_{PATHWISE}$ (Fig. 5b and c), which means that euprimates dispersed longer distance when the *LT* and *LP* changed at faster rates, irrespective if the changes were to warmer or colder temperatures, or to drier or wetter conditions. On the other hand, the LP_{RATE} had a significant positive effect on $NC_{PATHWISE}$ (Fig. 5f, Extended Data Table 3), explaining 14% of the variance (Extended Data Table 4). Therefore, euprimates diverged into new species more frequently when the total amount of annual *LP* changed at faster rates. This means that when the local environment became drier or wetter, rapidly over time, ancestral species speciated at faster rates.

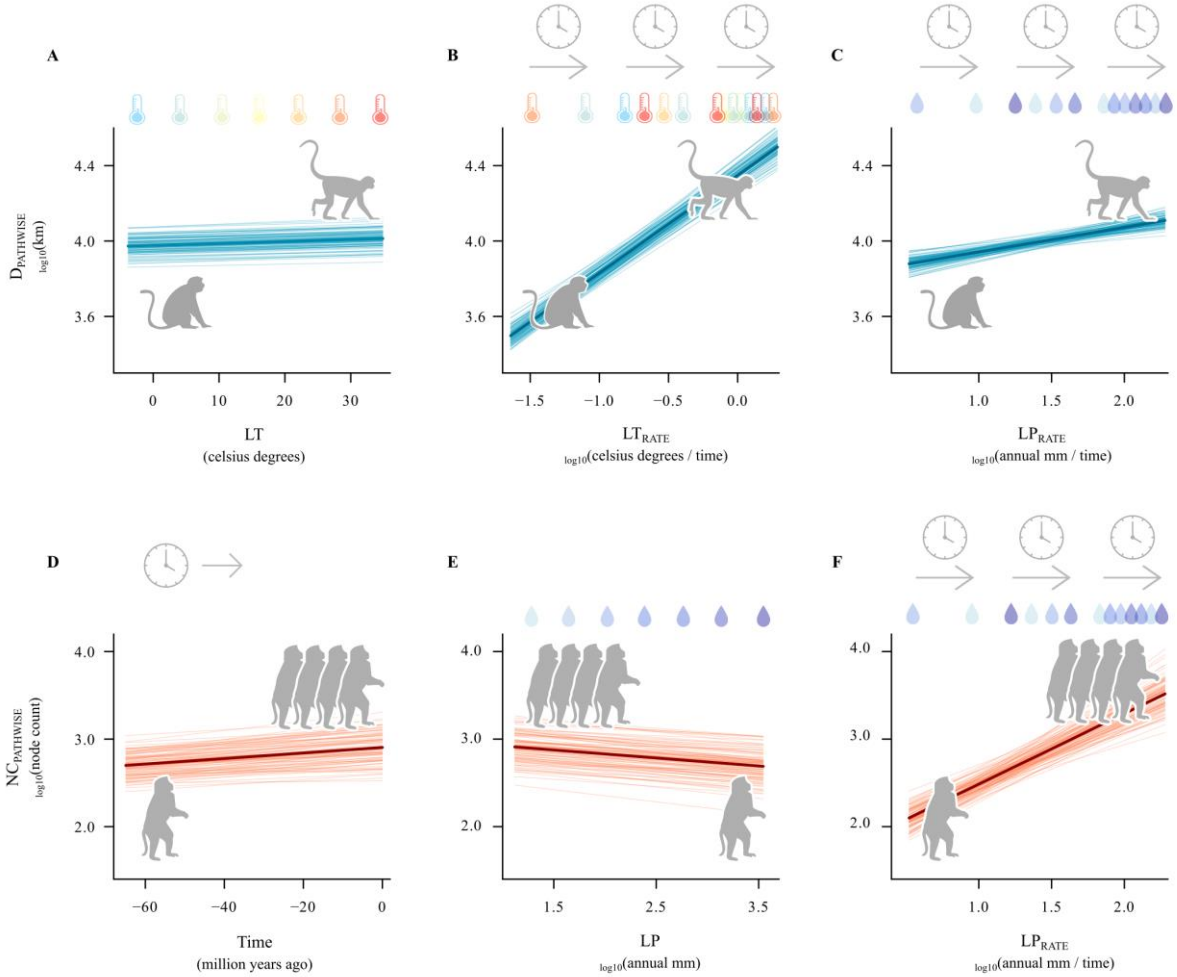

Figure 5. Euprimates dispersed and radiated under variable rates of change in local climate. (A) local temperature (LT) had a significant positive effect on pathwise distance ($D_{PATHWISE}$). (B) the pathwise rate of local temperature (LT_{RATE}) had a significant positive effect on $D_{PATHWISE}$. (C, F) the pathwise rate of local precipitation (LP_{RATE}) had a significant positive effect on both $D_{PATHWISE}$ and pathwise node count ($NC_{PATHWISE}$). (D) $NC_{PATHWISE}$ was positively associated with time. (E) local precipitation (LP) had a significant negative effect on $NC_{PATHWISE}$. We show the predictor variables that were significant in both the median and the sample of phylogenetic trees (see Methods). Light-coloured lines represent the posterior distribution of phylogenetic regression slopes. Darker lines represent the mean slopes of the posterior distribution.

The positive effect of LT_{RATE} and LP_{RATE} on dispersal and speciation was robust to several sources of uncertainty (see Methods, robustness of results section). These sources of uncertainty include the inferred ancestral locations reconstructed at every phylogenetic node (Extended Data Table 6 and 7), the multiple

continents proposed for the origin of the common ancestor (Extended Data Table 2), the spatial variation in *LT* and *LP* (Extended Data Table 6 and 7), and, principally, the topology and divergence times of the phylogenetic tree used in this study (Extended Data Table 6 and 7).

Conclusion

This study presents a novel view of euprimates biogeographic and evolutionary history. This novel view highlights the idea that the prevalence of extant species highly adapted to the warm and stable tropical climate are the result of a long evolutionary process that started by selection on ancestral species thriving in a variety of colder and more seasonal palaeo climates of the northern latitudes (Fig. 2 and 3). From this colder and more seasonal local palaeo environmental setting, the surviving species that started to expand taxonomically were those species able to disperse longer geographic distances, toward different but more stable climates (Fig. 3). The potential main selective force on dispersal ability was the rate of local environmental changes (LT_{RATE} and LP_{RATE}), as those variables substantially predicted dispersal distance (Extended Data Table 3).

With that in mind, we can logically hypothesize that the evolutionary failure of early euprimates (and Pleasiadapiformes, see Extended Data Fig. 1 and Table 5), living in the colder and more fluctuating climates of the northern continents, was caused by their inability to keep moving towards warmer and more stable climates. As the main factors driving species dispersal and speciation (i.e., LT_{RATE} and LP_{RATE}) were not directional, then early species did not become extinct from global cooling (i.e., directional climate change to lower global temperatures) or tropical rainforest contraction and disintegration in northern latitudes. Consequently, species with a higher capacity to disperse from places with challenging and volatile environments are the only ones that have left their evolutionary trace in contemporary Euprimate diversity.

Methods

Phylogenetic trees. Our comparative analyses were based on the most complete phylogeny of Euarchonta to date, which includes 902 tips of which 419 are extant and 483 are fossil species. The Euprimate clade (excluding the incertae sedis *Altanius orlovi* [14]) contains 404 extant and 361 fossil species. This phylogeny was reconstructed by Wisniewski et al. [28] who used a meta-analytical approach similar to matrix representation with parsimony super tree method. Their novel approach used a formal set of rules to accommodate phylogenetic uncertainty in source studies, removed redundant datasets or down-weighted datasets based on similar underlying matrices, and reconciled taxonomic information to a common source [28,65]. However, the phylogeny of Wisniewski et al. [28] has important sources of uncertainty such that the authors highlight several caveats before using the tree for comparative analyses. Principally, the fossil *Catarrhini indet CPI-6487*, caused the Wisniewski et al.'s "bizarre" reconstruction of South America as the continent of origin for the crown anthropoid ancestor (Catarrhini + Platyrrhini). Additionally, the median phylogenetic meta tree of Wisniewski et al. [28] contains 117 branches with zero length, which can be a source of bias in our comparative analyses.

To address those issues, we used a random sample of 100 of the total set of most parsimonious topologies (MPTs) obtained by Wisniewski et al. [28]. Additionally, as these topologies were undated, we accounted for uncertainty in branch length information by dating the sample using a tip-dating procedure adapted from that used by Wisniewski et al. [28]and implemented in BEAST2 [66]. We make just a few modifications to their procedure. Firstly, for each MPT, we restricted topology moves by setting the appropriate operators to have zero weight, to obtain a posterior distribution of trees with a single fixed topology but variation in divergence dates and branch lengths. We conditioned the fossilized birth-death process on the root, with a date calibration as described in Dos Reis et al. [67] ranging between 66 million years (the age of the oldest sampled fossil) and 130 million years (an absence of placental mammals). We additionally tested a model which calibrated on the origin of the birth-death process (using the same dates) but found no difference in the results. We set an exponential (mean =1) prior on the sigma parameter for the log-normal rate distribution applied to estimate optimized relaxed clock rates, as recommended for groups with clock-like rates of molecular evolution – supported in the molecular data underlying this analysis [67]. We restricted the mean clock rate to vary between 0.01 and 0.02 (extending beyond the extremes of variation observed in Wisniewski et al. [28] to facilitate faster convergence (though our results are identical when this parameter was not restricted). For transition rates we place a gamma prior (α= 0.2, β = 0.5) and for transversion rates a gamma prior (α= 0.2, β = 0.25); this avoids the default priors which place a lot of weight on very small values. Finally, we place a uniform prior ranging between 0 and 1 on the turnover rate and a beta distribution on the sampling proportion (α = 5, β=90). As BEAST2 does not work with multifurcations, all polytomies were randomly resolved before tip-dating; they were collapsed back to reflect the original input topology afterwards.

We removed three fossils (Cercopithecini sp. Indet. AUH 1321, Colobinae indet. KNM-BN 1251, and Colobinae indet. KNM-TH 48368) from our dated phylogenetic trees. As these taxa had uncertain placement (see [28]), our preliminary analyses indicated that divergence dates were being heavily influenced (varying by tens of millions of years) by their inclusion (along with Catarrhini indet CPI-6487, see above). We also excluded four taxa from the analyses because their taxonomic relationships were particularly problematic or because we could not identify the specimen when these tips had the genus name only. These four tips are Cantius UM 86543, Cheracebus purinus, Tupaia sp. UNSM 87244, and Dermoptera indet. Pkg 240 and Pkg 335. Finally, we edited 19 extant species names in the tree to match them with the IUCN Red List of Threatened Species [68] taxonomic nomenclature, and we edited seven extinct species names to match them with the Paleobiology Database (PBDB) taxonomic nomenclature (Extended Data Table 1).

For each of the 100 MPTs, we obtained a single representative dated phylogeny from our posterior distribution by calculating a median tree using the Kendall-Colijn metric [69]. This sample of trees contains 894 Euarchonta's tips (Supplementary Data S1). We also obtained a single representative tree by getting the median Kendall-Colijn tree from the sample of 100 median trees (Supplementary Data S2). We conducted the main comparative analyses based on the median tree and the sample of 100 median trees. We also conducted all the comparative analyses after excluding *Parvimico materdei*, *Dolichocebus annectens*, and *Ucayalipithecus perdita* as they (probably erroneously) were recovered as stem anthropoids [28]. Finally, we conducted all the comparative analyses on the original median tree available in Wisniewski et al. [28]. Results across all those multiple phylogenies were qualitatively similar (see Robustness of results section).

Geographic distribution data. We searched geographic coordinate data (longitude and latitude) for every tip in our median tree to infer the posterior distribution of ancestral coordinates across phylogenetic nodes. We obtained those coordinates by means of two different approaches for extant and extinct species.

For extant species, we downloaded the distribution polygons from the IUCN Red List of Threatened Species [68] and then we generated a random sample of coordinates within each polygon. This approach allowed us to get more information about the extent of the geographic distribution for each species than when using the observed geographic occurrences for each species or the distribution centroids. There were three species absent in the IUCN Red List database (i.e., *Lepilemur mittermeieri*, *Microcebus mittermeieri*, and *Otolemur crassicaudatus*), so we obtained their polygons using the Map of Life database instead [70]. We considered the polygons geographic area (in square kilometres) to define the number of random coordinates to be generated within them. Specifically, we generated n = 50, 100, 200, 300, 400, and 500 random coordinates, for polygons with km^2 = 20 – 100,000; 100,000 – 200,000; 200,000 - 300,000; 300,000 - 400,000; 400,000 - 500,000; and > 500,000, respectively. This data set is available as Supplementary Data S3.

For most fossil species, we downloaded their palaeogeographic coordinates from the PBDB. In the case of those fossil species that did not have information in the PBDB, we obtained their present-day coordinates from the localities where the fossils were found. Then, we reconstructed their palaeogeographic coordinates using the "reconstruct" function of the chromosphere R package, version 0.4.1[71]. We reconstructed the palaeogeographic coordinates based on the PALEOMAP model [72]. We additionally used the ages of both their first appearance datum (FAD) and last appearance datum (LAD) to reconstruct their palaeogeographic coordinates.

After getting the coordinates for all the tips in the median tree, we checked whether there were duplicated coordinates between sister species and for duplicated coordinates between each of the sister species and the closest single species to them. Then, we checked for coordinates between sister species whose Great Circle geographic distance was lower than 50 meters. We applied these procedures because preliminary analyses using the Geo model, with variable rates, collapsed the branches of those pair of tips (i.e., sister tips with either duplicated coordinates and/or geographic distances < 50 m) to zero lengths.

We found 10 fossils that matched the above-mentioned filtering criteria. However, to keep these fossils in the median tree, we conducted an alternative approach that generated random coordinates for them. Namely, we created a circular polygon of 0.5 kilometres of radius from the central palaeogeographic point where the fossil was found, and we generated 50 random coordinates within every circular polygon. The complete coordinate data set for fossils is available as Supplementary Data S4.

Ancestral locations inference. After getting the sample of geographic coordinates for each tip in the median tree, we inferred the posterior distribution of ancestral coordinates at every node in the median tree using a novel approach of the Geo (Geographical) model [33] in BayesTraits version 4 [34]. The previous version of the Geo model reconstructs the node posterior distribution of longitude and latitude onto a three-dimensional Cartesian

coordinates system, so that the model assumes that changes in coordinates occur onto a spherical space. The Geo model estimates the posterior distribution of ancestral coordinates while sampling across all the coordinates within phylogenetic tips – thus avoiding potential bias of using one coordinate per phylogenetic tip as geographic centroids, mid latitudes, or longitudes. Changes in coordinates across the branches of the phylogenetic tree are modelled using Brownian motion which assumes that species disperse across the globe at a constant speed (distance per time unite). However, the Geo model can also estimate ancestral locations while considering the continuous variation in dispersal speed across phylogenetic branches. The speed of movement ranges from species quiescence or no movement per time unit, through constant movement in direct proportion of the passage of time (Brownian motion), to long distance dispersal per time unit. Estimations of the variation in species dispersal speed across phylogenetic branches are based on the variable rate model [73]. The variable rate model detects shifts away from a (background) constant-rate of change in species geographic locations, expected under Brownian motion. We compared the constant and variable speed models by means of Bayes Factors (BF). The BF takes the model marginal likelihood for comparison which is estimated by the steppingstone sampling in BayesTraits. The steppingstone sampling estimated the model marginal likelihood while considering the number of parameters of the model (i.e., model complexity) [53]. The BF is calculated as the double of the difference between the log marginal likelihood of two models. Higher values of the log marginal likelihood represent better fitted models and, by convention, BF > 2 indicates positive support, BF = 5–10 indicates strong support, and BF > 10 is considered very strong support for a model over the other [74].

In this study we introduce a novel Geo model, which restricts reconstructed locations to points found only on land, this is an extension to the model developed by O'Donovan et al [33]. Initially reconstructed locations are placed on land, when proposing a new location, the closest point to the proposed location is identified on the map, if the closest point is found to be in the sea, the new location is assigned as zero probability (rejected), otherwise it is accepted or rejected based on its likelihood. Geography is not static through time, maps were created for different time periods (see below), as the phylogeny is time calibrated each internal node is assigned a map based on its age.

To restrict the space for ancestral location inferences across phylogenetic nodes, we used the global maps of the PALEOMAP project [72]. The PALEOMAP project contains global maps for every million years, during the past 1,100 million years. We matched every phylogenetic node with the closet palaeo map given their ages. With this approach we ensured that the reconstructed longitudes and latitudes for the phylogenetic internal nodes fell within the ancestral configuration of continents. This means that, for the first time, we could consider continental drift in the reconstruction of the primates' ancestral geographic locations.

We ran 10 MCMC chains of 800,000,000 million iterations each, discarding the first 600,000,000 million iterations as burn in. We also ran four analyses where we restricted the palaeo map for the node representing the crown Euprimate. We selected the four continents proposed as the ancestral location for the crown Euprimate: Asia, Africa, Europe, North America. We ran 10 MCMC chains of 800,000,000 million iterations for each of the four model restrictions, discarding the first 600,000,000 million iterations as burn in. Then we compared all the Geo models by means of Bayes Factor using the model marginal likelihood estimated by steppingstones. Usually, when Europe is suggested as the place of origin for the common ancestor of euprimates, it is implicitly included within the coarser continental area Eurasia [27,28]. This coarse discretization of Earth is a common practice given the limitations of biogeographical models that use discrete tip data in the phylogenetic tree. However, we leverage on the higher geographical resolution of the Geo model to evaluate any region within Eurasia as the likely location for crown euprimates.

Annual monthly palaeoprecipitation and palaeotemperature. We obtained global values of monthly precipitation and mean monthly surface temperature for a period spanning the entire evolutionary history of Euarchonta in the median and sample of phylogenetic trees, i.e., about 76 million years. We used three approaches to get the monthly precipitation and temperature for extant, fossil, and pseudo extinct (phylogenetic nodes) species, respectively.

First, for extant species, we extracted the monthly precipitation and temperature values from their geographic centroids. We estimated the species geographic centroid within their IUCN and MOL polygons, using the terra R package, version 1.7.71 (Supplementary Data S5). The data of monthly precipitation and temperature, at 30 second resolution, and ranging from the year 1970 to 2000, was extracted from the WordClim Version 2 [75].

Second, for fossil species (phylogenetic tips), we obtained the monthly palaeo precipitation and palaeo temperature values from their palaeo coordinates (Supplementary Data S4). To get the monthly palaeo

precipitation and palaeo temperature we used world palaeo climatic simulations based on the Hadley centre general circulation Coupled Model (HadCM3). Specifically, we used the Bristol Lower Ocean resolution (BL), MOSES2.1a land surface exchange scheme (M2.1a), and fully dynamic vegetation model (D) (i.e., HadCM3BL-M2.1aD model) [37–40]. The HadCM3BL-M2.1aD is a coupled General Circulation Model (GCM) that considers the coupled circulation of the atmosphere and ocean, land surface exchange scheme, and vegetation dynamics. We downloaded all the available monthly climatic layers in NetCDF format for 0 (the present), 4, 10, 14, 19, 25, 31, 35, 39, 44, 52, 55, 60, 66, 69, 75, and 80 million years ago. Then, we matched the fossil palaeo coordinates with the closet palaeo climate simulation layer, considering their ages. For fossil we used their FAD and LAD ages so that we can consider the uncertainty of age-matching as the palaeo climatic layers have a lower age resolution than the fossils ages.

Third, for the internal phylogenetic nodes (pseudo extinct species), we extracted the monthly palaeo precipitation and palaeotemperature from their posterior distribution of coordinates that were reconstructed with the Geo model. We used the monthly climatic data layers from the HadCM3BL-M2.1aD model, and we matched the posterior node coordinates with the closest palaeo climatic layer, given their ages. As there are many phylogenetic nodes in the median tree that do not match exactly the age of each climatic layer (given their difference in age resolution), we also extracted the palaeo climate data using the node ages from the sample of 100 phylogenetic trees. With this approach we considered the uncertainty in node ages when matching them with their closet simulated palaeo climate layers. All our results where qualitatively similar when running the analyses on the median tree and across the sample of 100 phylogenetic trees (see the Robustness of results section).

Köppen-Geiger climate classification. Using the monthly values of precipitation and mean monthly temperature for nodes, fossils, and extant species, we formally classified the climates based on the Köppen-Geiger climate classification system (KG). The KG system classifies climates into five main categories which are the Tropical (A), Arid (B), Temperate (C), Cold (D), and Polar (E) climates. Then, the KG system also classify the climates in 30 subcategories [44,45]. For example, within the main category Tropical, there exist the Tropical Rainfores, Tropical Savannah, and the Tropical Monson subcategories. Such classification is based on threshold values and annual seasonality of monthly precipitation and temperature [44]. It is important to note that the climate concept used in this study differs from the environment concept. Climates are first-order processes (i.e., processes that explain environment assuming a completely flat, non-variable landscape) for environments, but environments are also influenced by second-order processes such as focussed recharge, orography, topology, lithology etc. KG climates, for example, do not identify hydric wetlands and other microhabitat variability. Our approach allows us to separate the macro-scale first-order climatic processes influencing radiation and dispersal, but do not show fine detail environmental variability. We estimated the KG climate following the revised KG climate classification of Peel et al.'s [45] and using Wong Hearing et al.'s [41] R script.

The Extended Data Figure 2 show the world KG reconstructions for the present and for the past, using the WorldClim Version data, and the HadCM3BL-M2.1aD simulated palaeo climate data, respectively.

DPATHWISE. We obtained a measure for the geographic distance that each euprimate's species moved across the globe from the location of the MRCA. For this, we summed the dispersal distance on phylogenetic paths, i.e., across all phylogenetic branches that link the MRCA with every tip in the median tree. To get the geographic distance along paths we used a three-steps approach. First, we calculated the geographic distance per phylogenetic branch, using the Great Circle distance which is the shortest geographic distance between two geographic points on a spherical surface. As geographic points, we used the median of the coordinates that were inferred with the Geo model across phylogenetic nodes. Second, we calculated the Great Circle distance between the median posterior coordinate for the ancestral and descendant node per phylogenetic branch. For fossils and extant species, we obtained the median of the inferred palaeo coordinates and the within polygon centroid, respectively. Third, the summed the branch geographic distances along the paths that link the common ancestor with each fossil and extant species. This variable allows us to have a measure of the geographic distance that each fossil and extant species has moved over the globe since and from the origin of the common ancestor of the crown Euprimate (Supplementary Data S6).

NCPATHWISE. To study the correlates of speciation rates we used the node count (NC) along phylogenetic paths (Supplementary Data S6). There are alternatives non-model-based tip-rate metrics used to study the speciation rate correlates, such as the inverse of equal splits (ES) or the inverse of terminal branch length (TB). However, we preferred to use NC as it has been shown to be the speciation metric that is less influenced by potential biases and sources of uncertainty associated with branch-length estimation from empirical data [76]. NC captures the average speciation rate over the entire phylogenetic path and weight equally all branch lengths along the paths. We did not use tip-rate speciation metric estimated from time-varying birth–death diversification

models owing to the erroneous inference of the general diversification patterns when the variation in rate of sequence evolution is not properly considered during the time-tree inference [77], Additionally, it has also been shown in the context of phylogenetic regressions that NC is the response variable that exhibits the highest statistical power when compared to regressions using ES or TB as speciation metrics [49].

LP_{RATE} and LT_{RATE}. To quantify the rate of change in local precipitation and temperature for each species, we computed the total amount of change in local precipitation and local temperature on phylogenetic paths, and we divided this variable by the total time of each path given the time-calibrated median tree (Supplementary Data S6). To get the total amount of change along paths we used a three-steps approach. First, we extracted the local precipitation (LP) and local temperature (LT), from the posterior coordinates of each phylogenetic node, and from the palaeo coordinates for fossils and the geographic centroid for extant species. Second, we calculated the difference of the median LP and LT, between the ancestral and descendant node per phylogenetic branch. Third, we summed all the per branch differences between LP and LT, along the paths that link the common ancestor with each fossil and extant species and divided this variable by the total time of each path given the median time-calibrated phylogenetic tree.

Phylogenetic regressions. We performed two sets of phylogenetic regression analyses to study the correlates of $D_{PATHWISE}$ and $NC_{PATHWISE}$. To study the correlates of $D_{PATHWISE}$ we used Bayesian Phylogenetic Generalized Least Squares regression models (PGLS), estimating Pagel's lambda in BayesTraits v4.

We first evaluated the effect of time and global average temperature (GT) on $D_{PATHWISE}$. Time was obtained from the path length of the time-calibrated median phylogenetic tree (Supplementary Data S6). GT is available across the Phanerozoic in a resolution of one million year and was obtained from [47]. We extracted the GT from all the palaeo coordinates (given their FAD and LAD) for fossil tips, and from the centroid within the polygon for extant species (Supplementary Data S6). We matched the fossils and extant coordinates with the GT values, according to their age.

Then, we evaluated the effect of local precipitation (LP) and local temperature (LT) on $D_{PATHWISE}$. The LP and LT variables correspond to the annual precipitation and annual mean temperature values extracted from all the palaeo coordinates for fossil tips (given their FAD and LAD), and from the centroid within the polygon for extant species (Supplementary Data S6). The annual precipitation and annual mean temperature for fossils tips was extracted from the HadCM3BL-M2.1aD simulations layers. The annual precipitation and annual mean temperature for extant species was extracted from the WorldClim version 2 data. Finally, we evaluated the effect of LP_{RATE} and LT_{RATE} on $D_{PATHWISE}$.

To study the correlates of $NC_{PATHWISE}$ we performed Phylogenetic Generalized Linear Mixed models (PGLMM) using the MCMCglmm R package 2.35 [50]. We used a Poisson distribution to model $NC_{PATHWISE}$. As in the PGLS analyses $D_{PATHWISE}$, we tested the effect of time, GT, LP, LT, LP_{RATE}, and LT_{RATE}.

For the PGLS regression we ran 1,100,000 iterations, sampling every 1,000 iterations and discarding the first 100,000 iterations as burn in. Statistical significance of predictor variables was estimated based on a P_{MCMC} metric. This metric is based on counting the percentage of regression parameters that are higher (or lower) than zero in the posterior distribution. When the regression parameter is higher (or lower) than zero over 95% of the posterior distribution, then the predictor variable is statistically significant. For PGLMM regressions we also ran 1,100,000 iterations, sampling every 1,000 iterations and discarding the first 100,000 iterations as burn in. Regression coefficients were judged to be significant according to the P_{MCMC} metric estimated by the "MCMCglmm" R function.

Robustness of results

Phylogenetic uncertainty. We evaluated the robustness of our results to several sources of uncertainty in our data. First, we evaluated the effect divergence times and topological uncertainty of our median phylogenetic tree (Supplementary Data S2) by running the Geo model analyses across the sample of 100 median phylogenetic trees (Supplementary Information Data 1). Regarding the pattern of climatic reconstruction, we obtained qualitatively similar results across the 100 phylogenetic trees (Supplementary Information Data 7). We also got the same climatic pattern on the sample of trees that excluded the potentially problematic tips *Parvimico materdei*, *Dolichocebus annectens*, and *Ucayalipithecus perdita* (Supplementary Data S8). We also got the same pattern of ancestral climates when using the original meta tree available by Wisniewski et al. [28] (Supplementary Data S9).

To evaluate the effect of phylogenetic uncertainty on our phylogenetic regressions results, we obtained all the response and predictor variables from each of the 100 trees in the sample. Those variables are the $D_{PATHWISE}$, $NC_{PATHWISE}$, LP_{RATE}, and LT_{RATE}, Then, we ran the phylogenetic regression across each of the 100 samples of trees. We obtained qualitatively similar results. The variable LT, LT_{RATE}, and LP_{RATE} stand as the main drivers of euprimates dispersal distance (Extended Data Table 5). The variables Time, LP, and LP_{RATE} stand as the main drivers for euprimates speciation rates (Extended Data Table 6).

Taphonomic bias. We evaluated whether the geographic overrepresentation of non-tropical fossils was biasing our inferences of ancestral climates by conducting sensitivity analyses. We ran the Geo model and classified the KG climates using several phylogenetic trees and data sets that were generated by sub sampling the non-tropical fossils (Supplementary Data S10). We first classified the KG climates for all the fossils palaeo coordinates. As done previously, we used the fossils FAD and LAD ages to match them with the closest monthly climatic layer of the HadCM3BL-M2.1aD palaeo climate model. The fossils climate classification given their FAD and LAD is available as Data 10.

Second, we selected one main KG climate for each fossil, for both their FAD and LAD. When having more than two main climates for one fossil, we selected the climate with highest representation. When we had two main climates, we selected a climate at random. The final data sets are available as Data 10 (Top fossil climates files).

Third, we randomly down sampled the non-tropical fossils until we obtained the same proportion of the tropical fossils. For the KG fossil classification given their FADs, we obtained 73 tropical fossils and 285 non-tropical fossils (Supplementary Data S10). Then, we obtained 10 random samples of non-tropical fossils with following sizes: 271, 249, 227, 205, 183, 161, 139, 117, 95, and 73 (same as tropical fossils). For the KG fossil classification given their LADs, we obtained 84 tropical fossils and 274 non-tropical fossils (Supplementary Data S10). So, we obtained 10 random samples of non-tropical fossils with following sizes: 264, 244, 224, 204, 184, 164, 144, 124, 104, and 84 (same as tropical fossils). Such down-sampling procedure, given the FAD and LAD ages, was replicated 10 times, meaning that we analyzed 200 data set in total (Supplementary Data S10).

If the fossil data was biasing the climate reconstruction of early euprimates, we should observe an increase in the number of tropical climates in early phylogenetic nodes as we decrease the representation of non-tropical fossils. Contrary to this expectation, the results show that there was an enduring major representation of non-tropical climates across all nodes corresponding to early euprimates history, across all the 200 data sets (Supplementary Data S11). This means that, even when the input data sets for the Geo model analyses are heavily biassed towards tropical fossils, our inferred pattern of ancestral climates is maintained. Furthermore, the ancestral location for the crown Euprimate was inferred to be North America in 80% of those 200 data sets (Supplementary Data S11).

General circulation model. As our KG climates reconstructed across phylogenetic nodes are dependent on the simulation based on the HadCM3BL-M2.1aD model which have error associated and have a coarse temporal resolution, we reconstructed ancestral climates at phylogenetic nodes based on an independent approach. We estimated ancestral climates using the continuous time Markov model with variable transition rates in BayesTraits v4. For this, we used the observed KG climates observed in the extant species and fossil tips, categorizing then the climate with four states: Tropical, Arid, Temperature, and Cold. We estimated the ancestral climate by maximum likelihood in our median tree, and in each of the 100 trees in the sample. Then, we represented the climate for each node by picking the state with the highest likelihood. Finally, we compared these estimations with the estimation based on the HadCM3BL-M2.1aD across all phylogenetic nodes (see Extended Data Figure 3).

Acknowledgments

We are grateful to Carolynne Roberts, Olivia Price, Kerry Stewart, Suzy White, George Butler, and Jacob Gardner, for helpful discussion. We would like to thank to Veri Lobos Haoa for her work with the figures in this article. This research was funded by the Leverhulme Trust Research Leadership Award, RL-2019-012.

Data availability statement

Data and code will be made publicly available upon publication of the article in a peer-reviewed journal.

References

1. Silcox, M. T. & López-Torres, S. Major Questions in the Study of Primate Origins. *The Annual Review of Earth and Planetary Sciences is online at earth.annualreviews.org* **45**, 113–150 (2017).

2. Cartmill, M. Rethinking Primate Origins. *Science (1979)* **184**, 436–443 (1974).

3. Cartmilll, M. New Views on Primate Origins. *Evol Anthropol* 105–111 (1992).

4. Sussman, R. W. *Primate Origins and the Evolution of Angiosperms*. *American Journal of Primatology* vol. 23 (1991).

5. Jablonski, N. G. Primate homeland: Forests and the evolution of primates during the Tertiary and Quaternary in Asia. in *Anthropological Science* vol. 113 117–122 (2005).

6. Fleagle, J. G. & Gilbert, C. C. The Biogeography of Primate Evolution: The Role of Plate Tectonics, Climate and Chance. in *Primate Biogeography Progress and Prospects* (eds. Lehman, S. M. & Fleagle, J. G.) 375–418 (2006).

7. Smith, T., Rose, K. D., Gingerich, P. D. & Sabloff, J. A. Rapid Asia-Europe-North America geographic dispersal of earliest Eocene primate Teilhardina during the Paleocene-Eocene Thermal Maximum. *Proc Natl Acad Sci U S A* **130**, 11223–11227 (2006).

8. Soligo, Christophe., Will, O. A., Tavaré, Simon., Marshall, C. R. & Martin, R. D. New Light on the Dates of Primate Origins and Divergence. in *Primate Origins - Adaptations and Evolution* (ed. Ravosa, M. J.) 29–49 (Springer, 2006).

9. Ross, C. F., Hall, M. I. & Heesy, C. P. Were Basal Primates Nocturnal? Evidence from Eye and Orbit Shape. in *Primate Origins - Adaptations and Evolution* (ed. Ravosa, M. J.) 233–256 (Springer, 2006).

10. Cartmill, M., Lemelin, P. & Schmitt, D. Primate Gaits and Primate Origins. in *Primate Origins - Adaptations and Evolution* (ed. Ravosa, M. J.) 403–435 (Springer, 2006).

11. Shea, B. T. Start Small and Live Slow: Encephalization, Body Size, and Life History Strategies in Primate Origins and Evolution. in *Primate Origins - Adaptations and Evolution* 583–623 (Springer, 2006).

12. Snodgrass, J. J., Leonard, W. R. & Robertson, M. L. Primate Bioenergetics: An Evolutionary Perspective. in *Primate Origins - Adaptations and Evolution* (ed. Ravosa, M. J.) 703–737 (Springer, 2006).

13. Stringer, C. & Andrews, P. *The Complete World of Human Evolution*. (Thames & Hudson Ltd., London, 2011).

14. Fleagle, J. G. *Primate Adaptation & Evolution*. (Academic Press, 2013).

15. Soligo, C. & Smaers, J. B. Contextualising primate origins - an ecomorphological framework. *J Anat* **228**, 608–629 (2016).

16. Williams, B. Effects of Climate Change on Primate Evolution in the Cenozoic. *Nature Education Knowledge* **7**, (2016).

17. Youlatos, D., Moussa, D., Karantanis, N. E. & Rychlik, L. Locomotion, postures, substrate use, and foot grasping in the marsupial feathertail glider Acrobates pygmaeus (Diprotodontia: Acrobatidae): Insights into early euprimate evolution. *J Hum Evol* **123**, 148–159 (2018).

18. Beard, K. C. *The Oldest North American Primate and Mammalian Biogeography during the Paleocene-Eocene Thermal Maximum*. www.pnas.org/cgi/content/full/ (2008).

19. Gingerich, P. D. Environment and evolution through the Paleocene-Eocene thermal maximum. *Trends in Ecology and Evolution* vol. 21 246–253 Preprint at https://doi.org/10.1016/j.tree.2006.03.006 (2006).

20. Cachel, S. *Fossil Primates*. (Cambridge University Press, 2015).

21. Soligo, C. Invading Europe: Did climate or geography trigger early eocene primate dispersals? in *Folia Primatologica* vol. 78 297–313 (2007).

22. Korasidis, V. A., Wing, S. L., Shields, C. A. & Kiehl, J. T. Global Changes in Terrestrial Vegetation and Continental Climate During the Paleocene-Eocene Thermal Maximum. *Paleoceanogr Paleoclimatol* **37**, (2022).

23. Pohl, A., Wong Hearing, T., Franc, A., Sepulchre, P. & Scotese, C. R. Dataset of Phanerozoic continental climate and Köppen–Geiger climate classes. *Data Brief* **43**, (2022).

24. Smith, T., Rose, K. D. & Gingerich, P. D. *Rapid Asia-Europe-North America Geographic Dispersal of Earliest Eocene Primate Teilhardina during the Paleocene-Eocene Thermal Maximum*. www.pnas.orgcgidoi10.1073pnas.0511296103 (2006).

25. Bloch, J. I., Silcox, M. T., Boyer, D. M. & Sargis, E. J. *New Paleocene Skeletons and the Relationship of Plesiadapiforms to Crown-Clade Primates*. www.pnas.org/cgi/content/full/ (2007).

26. Silcox, M. T. The Biogeographic Origins of Primates and Euprimates: East, West, North, or South of Eden? in *Mammalian Evolutionary Morphology: a Tribute to Frederick S. Szalay.* (eds. Dagosto, M. & Sargis, E.) 199–231 (Springer-Verlag, New York, 2008).

27. Springer, M. S. *et al.* Macroevolutionary Dynamics and Historical Biogeography of Primate Diversification Inferred from a Species Supermatrix. *PLoS One* **7**, (2012).

28. Wisniewski, A. L., Lloyd, G. T. & Slater, G. J. Extant species fail to estimate ancestral geographical ranges at older nodes in primate phylogeny. *Proceedings of the Royal Society B: Biological Sciences* **289**, (2022).

29. Beard, C. East of Eden at the Paleocene/Eocene boundary. *Science* vol. 295 2028–2029 Preprint at https://doi.org/10.1126/science.1070259 (2002).

30. Burgener, L., Hyland, E., Reich, B. J. & Scotese, C. Cretaceous climates: Mapping paleo-Köppen climatic zones using a Bayesian statistical analysis of lithologic, paleontologic, and geochemical proxies. *Palaeogeogr Palaeoclimatol Palaeoecol* **613**, (2023).

31. Rosas, A. *et al.* The scarcity of fossils in the African rainforest. Archaeo-paleontological surveys and actualistic taphonomy in Equatorial Guinea. *Hist Biol* **34**, 1582–1590 (2022).

32. Bernard, A. B. & Marshall, A. J. Assessing the state of knowledge of contemporary climate change and primates. *Evolutionary Anthropology* vol. 29 317–331 Preprint at https://doi.org/10.1002/evan.21874 (2020).

33. O'Donovan, C., Meade, A. & Venditti, C. Dinosaurs reveal the geographical signature of an evolutionary radiation. *Nat Ecol Evol* **2**, 452–458 (2018).

34. Pagel, M., Meade, A. & Barker, D. Bayesian estimation of ancestral character states on phylogenies. *Syst Biol* **53**, 673–684 (2004).

35. Simpson, G. G. Extinction. *Proc Am Philos Soc* **129**, 407–416 (1985).

36. Fleagle, J. G. & Gilbert, C. C. The Biogeography of Primate Evolution: The Role of Plate Tectonics, Climate and Chance. in *Primate biogeography. Progress and Prospects* (eds. Lehman, S. M. & Fleagle, J. G.) 1–535 (Springer New York, NY, 2006). doi:doi.org/10.1007/0-387-31710-4.

37. Pope, V. D., Gallani, M. L., Rowntree, P. R. & Stratton, R. A. The impact of new physical parametrizations in the Hadley Centre climate model: HadAM3. *Clim Dyn* **16**, 123–146 (2000).

38. Gordon, C. *et al.* The simulation of SST, sea ice extents and ocean heat transports in a version of the Hadley Centre coupled model without ¯ux adjustments. *Clim Dyn* **16**, 16–147 (2000).

39. Valdes, P. J. *et al.* The BRIDGE HadCM3 family of climate models: HadCM3@Bristol v1.0. *Geosci Model Dev* **10**, 3715–3743 (2017).

40. Valdes, P. J., Scotese, C. R. & Lunt, D. J. Deep ocean temperatures through time. *Climate of the Past* **17**, 1483–1506 (2021).

41. Wong Hearing, T. W. *et al.* Quantitative comparison of geological data and model simulations constrains early Cambrian geography and climate. *Nat Commun* **12**, (2021).

42. Ontiveros, D. E. *et al.* Impact of global climate cooling on Ordovician marine biodiversity. *Nat Commun* **14**, (2023).

43. Wilson, L. N. *et al.* Global latitudinal gradients and the evolution of body size in dinosaurs and mammals. *Nat Commun* **15**, (2024).

44. Beck, H. E. *et al.* Present and future köppen-geiger climate classification maps at 1-km resolution. *Sci Data* **5**, (2018).

45. Peel, M. C., Finlayson, B. L. & Mcmahon, T. A. *Updated World Map of the Köppen-Geiger Climate Classification Hydrology and Earth System Sciences Updated World Map of the Köppen-Geiger Climate Classification*. *Earth Syst. Sci* vol. 11 www.hydrol-earth-syst-sci.net/11/1633/2007/ (2007).

46. Yu, C. *et al.* Climate paleogeography knowledge graph and deep time paleoclimate classifications. *Geoscience Frontiers* **14**, (2023).

47. Scotese, C. R., Song, H., Mills, B. J. W. & van der Meer, D. G. Phanerozoic paleotemperatures: The earth's changing climate during the last 540 million years. *Earth Sci Rev* **215**, (2021).

48. Silvestro, D. *et al.* Early Arrival and Climatically-Linked Geographic Expansion of New World Monkeys from Tiny African Ancestors. *Syst Biol* **68**, 78–92 (2019).

49. Harvey, M. G. & Rabosky, D. L. Continuous traits and speciation rates: Alternatives to state-dependent diversification models. *Methods Ecol Evol* **9**, 984–993 (2018).

50. Hadfield, J. D. *MCMC Methods for Multi-Response Generalized Linear Mixed Models: The MCMCglmm R Package*. *JSS Journal of Statistical Software* vol. 33 http://www.jstatsoft.org/ (2010).

51. Morse, P. E. *et al.* New fossils, systematics, and biogeography of the oldest known crown primate Teilhardina from the earliest Eocene of Asia, Europe, and North America. *J Hum Evol* **128**, 103–131 (2019).

52. Gebo, D. L., Smith, R., Dagosto, M. & Smith, T. Additional postcranial elements of Teilhardina Belgica: The oldest European primate. *Am J Phys Anthropol* **156**, 388–406 (2015).

53. Xie, W., Lewis, P. O., Fan, Y., Kuo, L. & Chen, M. H. Improving marginal likelihood estimation for bayesian phylogenetic model selection. *Syst Biol* **60**, 150–160 (2011).

54. Clarke, A. *Principles of Thermal Ecology. Temperature, Energy and Life*. (Oxford University Press, 2017). doi:DOI 10.1093/oso/9780199551668.001.0001.

55. Zhang, J. *et al.* Modeling the effects of global cooling and the Tethyan Seaway closure on North African and South Asian climates during the Middle Miocene Climate Transition. *Palaeogeogr Palaeoclimatol Palaeoecol* **619**, (2023).

56. Zhang, Z. *et al.* Aridification of the Sahara desert caused by Tethys Sea shrinkage during the Late Miocene. *Nature* **513**, 401–404 (2014).

57. Zachos, J., Pagani, H., Sloan, L., Thomas, E. & Billups, K. Trends, rhythms, and aberrations in global climate 65 Ma to present. *Science (1979)* **292**, 686–693 (2001).

58. Pagel, M. Detecting correlated evolution on phylogenies: a general method for the comparative analysis of discrete characters. *Proc R Soc Lond B Biol Sci* **255**, 37–45 (1994).

59. Johnson, K. R. & Ellis, B. A Tropical Rainforest in Colorado 1.4 Million Years After the Cretaceous-Tertiary Boundary. *Science (1979)* **296**, 2379–2383 (2002).

60. Zhang, L. *et al.* Global assessment of primate vulnerability to extreme climatic events. *Nat Clim Chang* **9**, 554–561 (2019).

61. Sales, L., Ribeiro, B. R., Chapman, C. A. & Loyola, R. Multiple dimensions of climate change on the distribution of Amazon primates. *Perspect Ecol Conserv* **18**, 83–90 (2020).

62. Pinto, M. P., Beltrão-Mendes, R., Talebi, M. & de Lima, A. A. Primates facing climate crisis in a tropical forest hotspot will lose climatic suitable geographical range. *Sci Rep* **13**, (2023).

63. Qi, X. G. *et al.* Adaptations to a cold climate promoted social evolution in Asian colobine primates. *Science (1979)* **380**, (2023).

64. Kamilar, J. M. & Beaudrot, L. Effects of Environmental Stress on Primate Populations. (2018) doi:10.1146/annurev-anthro-102317.

65. Lloyd, G. T. & Slater, G. J. A Total-Group Phylogenetic Metatree for Cetacea and the Importance of Fossil Data in Diversification Analyses. *Syst Biol* **70**, 922–939 (2021).

66. Bouckaert, R. *et al.* BEAST 2: A Software Platform for Bayesian Evolutionary Analysis. *PLoS Comput Biol* **10**, (2014).

67. Dos Reis, M. *et al.* Using phylogenomic data to explore the effects of relaxed clocks and calibration strategies on divergence time estimation: Primates as a test case. *Syst Biol* **67**, 594–615 (2018).

68. IUCN. The IUCN Red List of Threatened Species. Version 2022-2. https://www.iucnredlist.org. Accessed on [07/11/2022]. 2022 (2022).

69. Kendall, M. & Colijn, C. Mapping Phylogenetic Trees to Reveal Distinct Patterns of Evolution. *Mol Biol Evol* **33**, 2735–2743 (2016).

70. Jetz, W., McPherson, J. M. & Guralnick, R. P. Integrating biodiversity distribution knowledge: Toward a global map of life. *Trends Ecol Evol* **27**, 151–159 (2012).

71. Kocsis, Á. T. & Raja, N. B. chronosphere: Earth system history variables. (2020) doi:10.5281/zenodo.3530703.

72. Scotese, C. R. & Wright, N. PALEOMAP Paleodigital Elevation MOdels (PaleoDEMS) for the Phanerozoic PALEOMAP Project, EarthByte.

73. Venditti, C., Meade, A. & Pagel, M. Multiple routes to mammalian diversity. *Nature* **479**, 393–396 (2011).

74. Raftery, A. E. Hypothesis testing and model selection. in *Markov Chain Monte Carlo in Practice* (eds. Gilks, W., Richardson, S. & Spiegelhalter, D.) 163–187 (Chapman & Hall, London, 1996).

75. Fick, S. E. & Hijmans, R. J. WorldClim 2: new 1-km spatial resolution climate surfaces for global land areas. *International Journal of Climatology* **37**, 4302–4315 (2017).

76. Title, P. O. & Rabosky, D. L. Tip rates, phylogenies and diversification: What are we estimating, and how good are the estimates? *Methods Ecol Evol* **10**, 821–834 (2019).

77. Shafir, A., Azouri, D., Goldberg, E. E. & Mayrose, I. Heterogeneity in the rate of molecular sequence evolution substantially impacts the accuracy of detecting shifts in diversification rates. *Evolution (N Y)* (2020) doi:https://doi.org/10.1111/evo.14036.

Extended Data

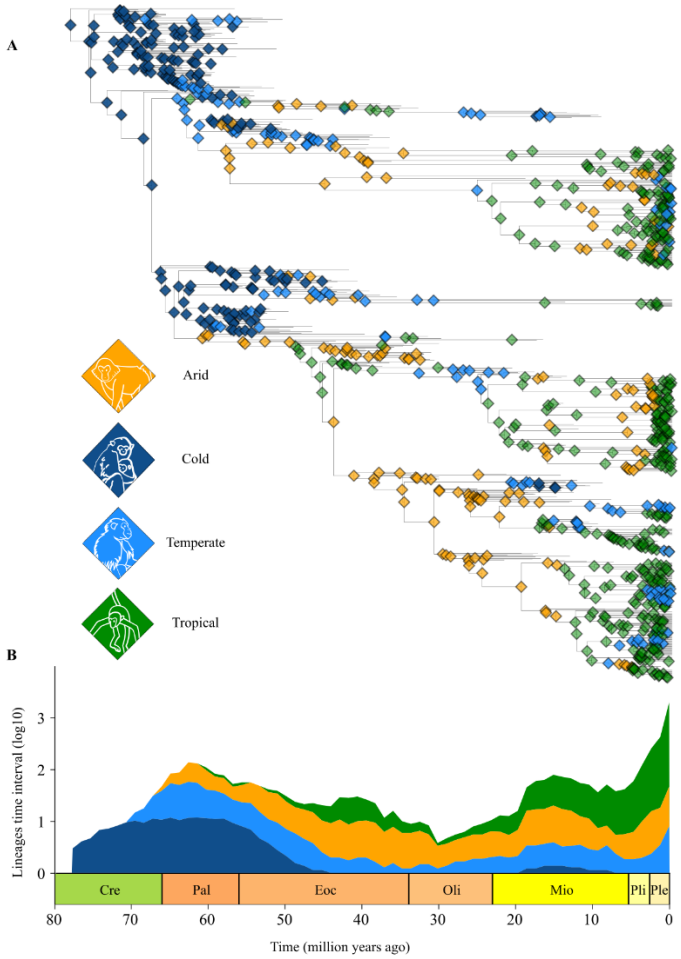

Extended Data Figure 1. Ancestral Plesiadapiformes and Euprimates inhabited diverse climates. A. Primates (Euprimates and Plesiadapiformes) phylogenetic tree with the Köppen-Geiger main climates categories for all nodes. The climate reconstruction was obtained by using the Geo model posterior coordinates and extracting the monthly palaeotemperature and precipitation simulated HadCM3BL-M2.1aD. B. lineages through time intervals of one million years, which additionally considers the tip climates. Colors represent the relative proportion of lineages inhabiting each climate category.

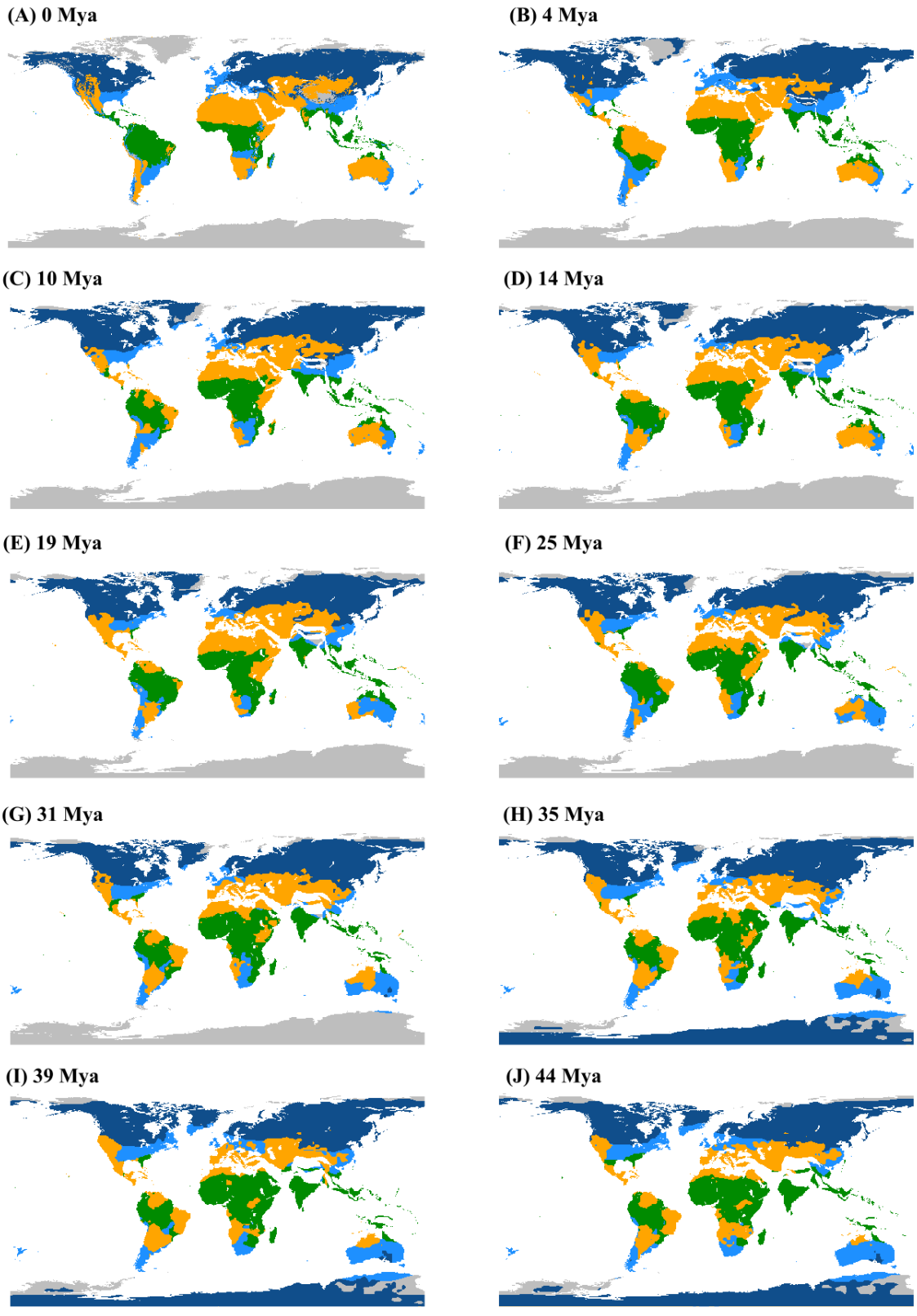
(A) 0 Mya
(B) 4 Mya
(C) 10 Mya
(D) 14 Mya
(E) 19 Mya
(F) 25 Mya
(G) 31 Mya
(H) 35 Mya
(I) 39 Mya
(J) 44 Mya
Koppen-Geiger main climate category
Tropical
Arid
Temperate
Cold
Polar

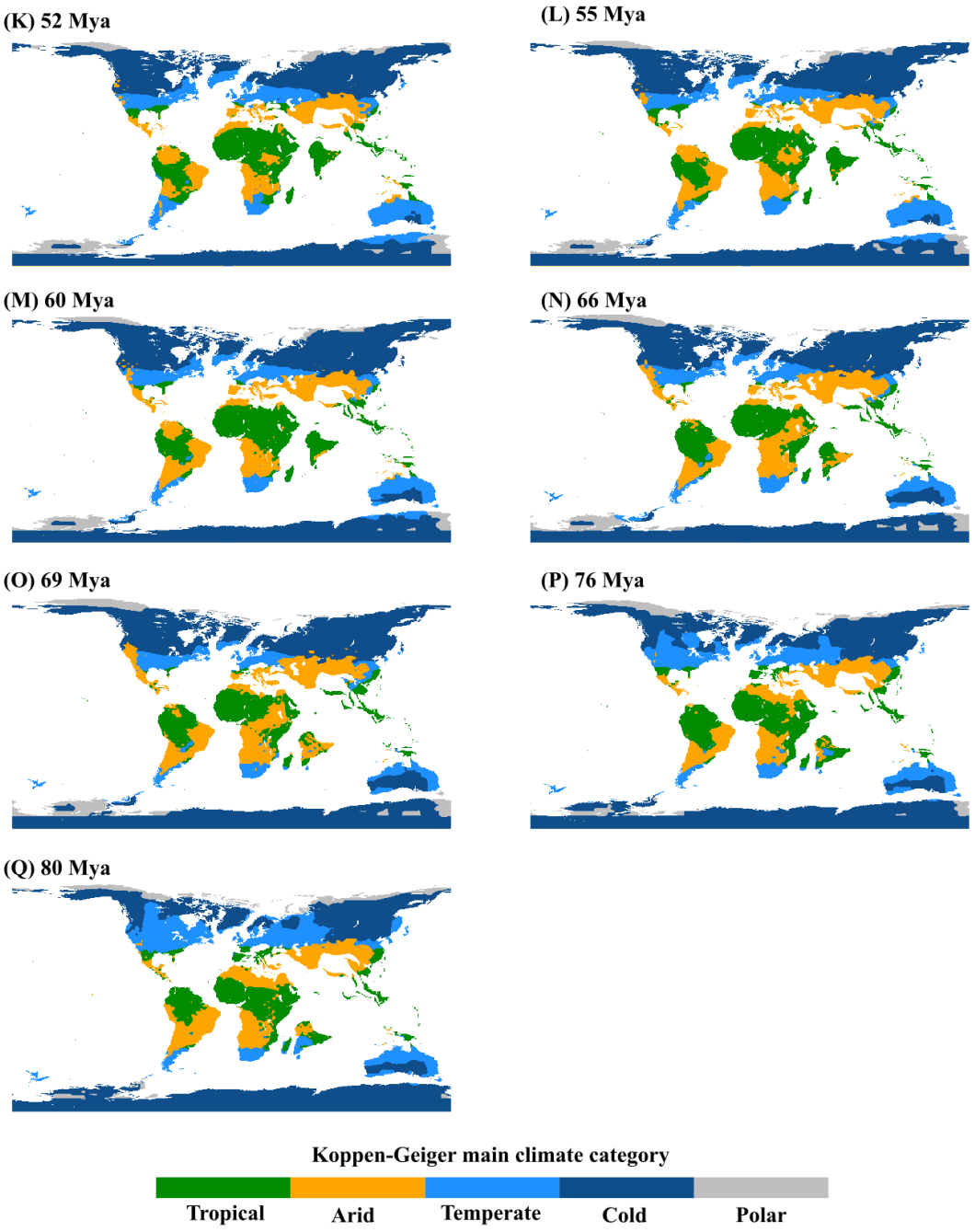

Extended Data Figure 2. Global Koppen-Geiger main climate reconstructions. **A.** Climates from the present were reconstructed using the WorldClim version 2 monthly data. **B-Q.** All other paleo climates were reconstructed based on the simulated climate data from the HadCM3BL-M2.1aD general circulation model.

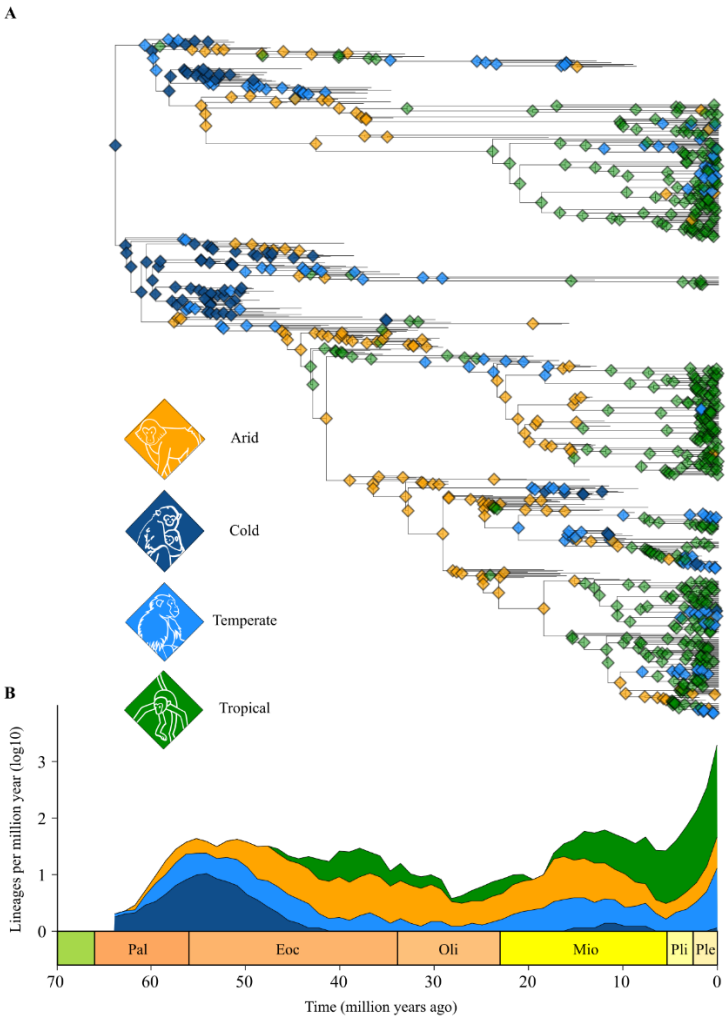

Extended Data Figure 3. Ancestral climates reconstructed with the Mk model for discrete trait evolution, using the climates for extant and fossils tips as input data. **A.** Euprimate phylogenetic tree with the Köppen-Geiger main climates categories for all nodes. We show the climate with the highest likelihood per node. **B.** lineages through time intervals of one million years. Colors represent the relative proportion of lineages inhabiting each climate category. Please see Figure 3 in the main text for comparison with the ancestral climates reconstructed based on the Geo model and the GCM.

Extended Data Table 1.
Edited tip-names in the Euarchonta median tree.

MCC tree name	MCC tree dited name	Justification
Alouatta_coibensis	Alouatta_palliata_coibensis	Subspecies in the IUCN Red List
Alouatta_palliatus	Alouatta_palliata_palliata	Subspecies in the IUCN Red List
Avahi_betsilio	Avahi_betsileo	Typo
Avahi_ramanantsoavani	Avahi_ramanantsoavanai	Typo
Cercopithecus_albogularis	Cercopithecus_mitis_albogularis	Subspecies in the IUCN Red List
Cercopithecus_doggetti	Cercopithecus_mitis_doggetti	Subspecies in the IUCN Red List
Cercopithecus_dryas	Chlorocebus_dryas	Synonym in the IUCN Red List
Cercopithecus_kandti	Cercopithecus_mitis_kandti	Subspecies in the IUCN Red List
Chiropotes_israelita	Chiropotes_sagulatus	Synonym in the IUCN Red List
Lagothrix_cana	Lagothrix_lagothricha_cana	Subspecies in the IUCN Red List
Lagothrix_lagotricha	Lagothrix_lagothricha_lagothricha	Subspecies in the IUCN Red List
Lagothrix_lugens	Lagothrix_lagothricha_lugens	Subspecies in the IUCN Red List
Lagothrix_poeppigii	Lagothrix_lagothricha_poeppigii	Subspecies in the IUCN Red List
Lepilemur_sahamalazensis	Lepilemur_sahamalaza	Synonym in the IUCN Red List
Lepilemur_wrighti	Lepilemur_wrightae	Synonym in the IUCN Red List
Mico_humeralifera	Mico_humeralifer	Synonym in the IUCN Red List
Mico_humilis	Callibella_humilis	Synonym in the IUCN Red List
Otolemur_monteiri	Otolemur_crassicaudatus_argentatus	Monteiri and argentatus are synonyms and sub species of crassicaudatus but only argentatus has IUCN data.
Saguinus_graellsi	Leontocebus_nigricollis_graellsi	Synonym and subspecies in the IUCN Red List.
Theropithecus_sp_M2974_et_MP44	Theropithecus_darti	Synonym PBDB.
AnchomomysFendantia_pygmaeus	Anchomomys_(Fendantia)_pygmaeus	PBDB format-compatibility
AnchomomysHuerzeleris_quercyi	Anchomomys_(Huerzeleris)_quercyi	PBDB format-compatibility
HispanopithecusHispanopithecus_hungaricus	Hispanopithecus_(Hispanopithecus)_hungaricus	PBDB format-compatibility
HispanopithecusHispanopithecus_laietanus	Hispanopithecus_(Hispanopithecus)_laietanus	PBDB format-compatibility
LeptadapisParadapis_priscus	Leptadapis_(Paradapis)_priscus	PBDB format-compatibility
TheropithecusOmopithecus_brumpti	Theropithecus_(Omopithecus)_brumpti	PBDB format-compatibility

Extended Data Table 2.
Geographic location of crown Euprimates inferred across a sample of 100 phylogenetic trees.

Sample Tree	Crown Euprimates Node Age	Restriction World Paleo Map Age	Median Posterior Longitude	Median Posterior Latitude	Paleo Continent
1	64.43	64	8.00	44.27	Europe
2	63.77	64	-79.34	51.99	North America
3	63.43	63	7.78	44.44	Europe
4	65.08	65	-77.04	52.44	North America
5	63.98	64	-78.90	52.81	North America
6	64.96	65	-78.30	52.46	North America
7	64.15	64	-80.13	52.13	North America
8	64.15	64	-77.87	52.42	North America
9	64.24	64	10.31	44.89	Europe
10	65.07	65	-78.92	52.09	North America
11	63.99	64	-79.71	52.33	North America
12	63.79	64	-79.39	52.14	North America
13	63.45	63	6.91	44.13	Europe
14	63.06	63	-80.15	51.98	North America
15	63.78	64	-79.34	51.83	North America
16	63.74	64	-80.31	51.82	North America
17	65.32	65	7.81	43.64	Europe
18	65.33	65	6.56	42.91	Europe
19	64.36	64	-78.28	52.70	North America
20	65.04	65	-79.70	51.88	North America
21	64.91	65	8.91	44.09	Europe
22	65.97	66	-79.18	52.11	North America
23	64.75	65	-78.42	52.05	North America
24	65.29	65	-78.72	51.94	North America
25	64.61	65	-79.02	52.01	North America
26	63.76	64	-79.37	51.99	North America
27	63.90	64	6.63	43.99	Europe
28	64.81	65	6.02	43.26	Europe
29	65.19	65	7.03	43.66	Europe
30	64.17	64	-80.15	52.26	North America
31	63.96	64	-78.74	52.22	North America
32	64.16	64	-79.50	51.84	North America

33	63.41	63	-76.63	52.47	North America
34	66.21	66	-77.83	52.15	North America
35	63.44	63	-77.61	52.90	North America
36	65.97	66	-79.69	52.32	North America
37	63.07	63	-78.37	51.98	North America
38	64.19	64	-75.57	51.78	North America
39	64.01	64	-78.83	52.11	North America
40	64.50	65	-77.42	53.74	North America
41	63.96	64	7.62	44.60	Europe
42	63.34	63	8.48	44.15	Europe
43	64.72	65	-78.54	52.14	North America
44	64.41	64	-78.36	51.67	North America
45	64.68	65	-79.51	52.15	North America
46	64.97	65	6.63	43.78	Europe
47	65.19	65	8.33	44.50	Europe
48	63.65	64	6.63	44.29	Europe
49	64.39	64	-78.92	52.29	North America
50	63.43	63	7.16	43.94	Europe
51	64.81	65	-79.06	51.81	North America
52	64.88	65	7.48	43.20	Europe
53	63.99	64	8.19	42.87	Europe
54	63.83	64	6.34	43.18	Europe
55	65.76	66	-79.92	52.14	North America
56	64.44	64	-79.41	51.94	North America
57	65.48	65	6.42	43.76	Europe
58	65.12	65	-76.12	52.53	North America
59	65.58	66	-77.65	52.41	North America
60	64.19	64	-77.43	52.40	North America
61	63.91	64	-74.99	52.92	North America
62	63.79	64	-80.47	52.00	North America
63	63.37	63	-77.69	52.44	North America
64	64.16	64	-78.99	52.42	North America
65	63.67	64	5.73	44.29	Europe
66	62.87	63	-75.84	52.40	North America
67	65.14	65	-80.18	52.07	North America
68	64.50	65	7.02	44.21	Europe

69	65.16	65	-78.48	51.93	North America
70	64.23	64	-79.66	52.32	North America
71	64.82	65	-79.15	52.11	North America
72	65.18	65	-77.57	52.36	North America
73	64.62	65	8.39	42.91	Europe
74	63.21	63	-79.52	52.27	North America
75	63.60	64	-78.22	51.61	North America
76	64.39	64	-79.70	51.77	North America
77	64.92	65	-12.93	58.96	Europe
78	63.22	63	6.52	44.30	Europe
79	65.62	66	-79.76	52.08	North America
80	64.84	65	-75.79	52.87	North America
81	65.06	65	6.05	43.10	Europe
82	63.87	64	6.35	44.30	Europe
83	64.03	64	-79.52	52.12	North America
84	64.15	64	-77.13	52.36	North America
85	64.52	65	-79.55	51.73	North America
86	64.65	65	-79.17	52.19	North America
87	65.36	65	9.54	43.85	Europe
88	63.71	64	3.15	42.79	Europe
89	64.49	64	-79.57	52.04	North America
90	64.46	64	-77.71	52.27	North America
91	64.07	64	-76.12	52.60	North America
92	64.54	65	-79.06	52.46	North America
93	65.14	65	-77.34	52.83	North America
94	65.11	65	-79.41	52.05	North America
95	63.35	63	-79.74	52.20	North America
96	65.02	65	-79.93	52.44	North America
97	64.37	64	-12.52	61.85	Europe
98	63.91	64	-79.68	52.18	North America
99	64.89	65	-79.09	52.25	North America
100	65.51	66	-79.07	52.22	North America

Extended Data Table 3.
Bayesian phylogenetic regression models predicting $D_{PATHWISE}$ and $NC_{PATHWISE}$ for Euprimates. Analyses are based on the median phylogenetic tree. The best-fit regression, given the marginal likelihood and deviance information criterion, for each response variable, is at the bottom. GT = Global temperature, LT = Local temperature, LT_{RATE} = Pathwise rate local temperature, LP = Local precipitation, LP_{RATE} = Pathwise rate local precipitation, DIC = Deviance information criterion, MLh = Marginal likelihood estimated by stepping-stones. Beta parameters in black color are significant, i.e., $P_{MCMC} < 0.05$. Beta parameters in grey color are not significant, i.e., $P_{MCMC} > 0.05$.

Response	**Predictors**	**DIC**	**MLh**	**R^2**
$D_{PATHWISE}$	$\beta_0 + \beta_1(Time) + \beta_2(GT)$	-	1448.32	0.07
	$\beta_0 + \beta_1(Time) + \beta_2(LT) + \beta_3(LP)$	-	1441.59	0.08
	$\beta_0 + \beta_1(Time) + \beta_2(LT) + \beta_3(LT_{RATE}) + \beta_4(LP_{RATE})$	-	1603.77	0.41
$NC_{PATHWISE}$	$\beta_0 + \beta_1(Time) + \beta_2(GT)$	4314.79	-	0.37
	$\beta_0 + \beta_1(Time) - \beta_2(LT) - \beta_3(LP)$	4313.48	-	0.37
	$\beta_0 + \beta_1(Time) - \beta_2(LT_{RATE}) + \beta_3(LP_{RATE})$	4290.25	-	0.50
	$\beta_0 + \beta_1(Time) + \beta_2(LP_{RATE})$	4289.05	-	0.49
	$\beta_0 + \beta_1(Time) - \beta_2(LT) - \beta_3(LP) + \beta_4(LP_{RATE})$	4281.92	-	0.51

Extended Data Table 4.
Effect size of the variables affecting Euprimates' $D_{PATHWISE}$ and $NC_{PATHWISE}$. R^2_{DELTA} is the effect size of each variable. Effect size was calculated from the difference between the R^2 of the regression containing all significant variables and the R^2 of the regression excluding the variable in question.

Response	**Variable**	**P_{MCMC}**	**R^2_{DELTA}**
$D_{PATHWISE}$	Time	0.004	0.004
	LT	0	0.015
	LT_{RATE}	0	0.19
	LP_{RATE}	0	0.021
$NC_{PATHWISE}$	Time	0.02	0.001
	LT	0.04	0.001
	LP	0.004	0.02
	LP_{RATE}	0	0.14

Extended Data Table 5.
Bayesian phylogenetic regression models predicting $D_{PATHWISE}$ and $NC_{PATHWISE}$ for Primates, i.e., Euprimates plus Plesiadapiformes. The best-fit regression, given the marginal likelihood and deviance information criterion, for each response variable, is at the bottom. GT = Global temperature, LT = Local temperature, LT_{RATE} = Pathwise rate local temperature, LP = Local precipitation, LP_{RATE} = Pathwise rate local precipitation, DIC = Deviance information criterion, MLh = Marginal likelihood estimated by stepping-stones. Beta parameters in black color are significant, i.e., $P_{MCMC} < 0.05$. Beta parameters in grey color are not significant, i.e., $P_{MCMC} > 0.05$.

Response	**Predictors**	**DIC**	**MLh**	**R^2**
$D_{PATHWISE}$	$\beta_0 + \beta_1(Time) + \beta_2(GT)$	-	761.84	0.06
	$\beta_0 + \beta_1(Time) + \beta_2(GT) + \beta_3(LT) + \beta_4(LP)$	-	767.09	0.11
	$\beta_0 + \beta_1(Time) + \beta_2(GT) + \beta_3(LT) + \beta_4(LT_{RATE}) + \beta_5(LP_{RATE})$	-	1199.41	0.68
$NC_{PATHWISE}$	$\beta_0 + \beta_1(Time) + \beta_2(GT)$	4920.33	-	0.43
	$\beta_0 + \beta_1(Time) + \beta_2(GT) + \beta_3(LT) - \beta_4(LP)$	4922.05	-	0.44
	$\beta_0 + \beta_1(Time) + \beta_2(GT) + \beta_3 (LT_{RATE}) + \beta_4(LP_{RATE})$	4864.24	-	0.61
	$\beta_0 + \beta_1(Time) + \beta_2(GT) + \beta_3(LP_{RATE})$	4862.87	-	0.61
	$\beta_0 + \beta_1(Time) + \beta_2(GT) - \beta_3(LT) + \beta_4(LP) + \beta_5(LP_{RATE})$	4856.98	-	0.62

Extended Data Table 6.
Phylogenetic regression predicting $D_{PATHWISE}$ across the sample of 100 phylogenetic trees of Euprimates. Beta parameters in black color are significant, i.e., $P_{MCMC} < 0.05$. Beta parameters in grey color are not significant, i.e., $P_{MCMC} > 0.05$.

Sample tree	Response	Predictors	R^2
1	$D_{PATHWISE}$	$\beta_0 + \beta_1(Time) + \beta_2(GT) + \beta_3(LT) + \beta_4(LP) + \beta_5(LT_{RATE}) + \beta_6(LP_{RATE})$	0.40
2	$D_{PATHWISE}$	$\beta_0 + \beta_1(Time) + \beta_2(GT) + \beta_3(LT) + \beta_4(LP) + \beta_5(LT_{RATE}) + \beta_6(LP_{RATE})$	0.67
3	$D_{PATHWISE}$	$\beta_0 + \beta_1(Time) + \beta_2(GT) + \beta_3(LT) + \beta_4(LP) + \beta_5(LT_{RATE}) + \beta_6(LP_{RATE})$	0.43
4	$D_{PATHWISE}$	$\beta_0 + \beta_1(Time) + \beta_2(GT) + \beta_3(LT) + \beta_4(LP) + \beta_5(LT_{RATE}) + \beta_6(LP_{RATE})$	0.51
5	$D_{PATHWISE}$	$\beta_0 + \beta_1(Time) + \beta_2(GT) + \beta_3(LT) + \beta_4(LP) + \beta_5(LT_{RATE}) + \beta_6(LP_{RATE})$	0.59
6	$D_{PATHWISE}$	$\beta_0 + \beta_1(Time) + \beta_2(GT) + \beta_3(LT) + \beta_4(LP) + \beta_5(LT_{RATE}) + \beta_6(LP_{RATE})$	0.71
7	$D_{PATHWISE}$	$\beta_0 + \beta_1(Time) + \beta_2(GT) + \beta_3(LT) + \beta_4(LP) + \beta_5(LT_{RATE}) + \beta_6(LP_{RATE})$	0.48
8	$D_{PATHWISE}$	$\beta_0 + \beta_1(Time) + \beta_2(GT) + \beta_3(LT) + \beta_4(LP) + \beta_5(LT_{RATE}) + \beta_6(LP_{RATE})$	0.67
9	$D_{PATHWISE}$	$\beta_0 + \beta_1(Time) + \beta_2(GT) + \beta_3(LT) + \beta_4(LP) + \beta_5(LT_{RATE}) + \beta_6(LP_{RATE})$	0.38
10	$D_{PATHWISE}$	$\beta_0 + \beta_1(Time) + \beta_2(GT) + \beta_3(LT) + \beta_4(LP) + \beta_5(LT_{RATE}) + \beta_6(LP_{RATE})$	0.62
11	$D_{PATHWISE}$	$\beta_0 + \beta_1(Time) + \beta_2(GT) + \beta_3(LT) + \beta_4(LP) + \beta_5(LT_{RATE}) + \beta_6(LP_{RATE})$	0.61
12	$D_{PATHWISE}$	$\beta_0 + \beta_1(Time) + \beta_2(GT) + \beta_3(LT) + \beta_4(LP) + \beta_5(LT_{RATE}) + \beta_6(LP_{RATE})$	0.63
13	$D_{PATHWISE}$	$\beta_0 + \beta_1(Time) + \beta_2(GT) + \beta_3(LT) + \beta_4(LP) + \beta_5(LT_{RATE}) + \beta_6(LP_{RATE})$	0.39
14	$D_{PATHWISE}$	$\beta_0 + \beta_1(Time) + \beta_2(GT) + \beta_3(LT) + \beta_4(LP) + \beta_5(LT_{RATE}) + \beta_6(LP_{RATE})$	0.65
15	$D_{PATHWISE}$	$\beta_0 + \beta_1(Time) + \beta_2(GT) + \beta_3(LT) + \beta_4(LP) + \beta_5(LT_{RATE}) + \beta_6(LP_{RATE})$	0.64
16	$D_{PATHWISE}$	$\beta_0 + \beta_1(Time) + \beta_2(GT) + \beta_3(LT) + \beta_4(LP) + \beta_5(LT_{RATE}) + \beta_6(LP_{RATE})$	0.56
17	$D_{PATHWISE}$	$\beta_0 + \beta_1(Time) + \beta_2(GT) + \beta_3(LT) + \beta_4(LP) + \beta_5(LT_{RATE}) + \beta_6(LP_{RATE})$	0.43
18	$D_{PATHWISE}$	$\beta_0 + \beta_1(Time) + \beta_2(GT) + \beta_3(LT) + \beta_4(LP) + \beta_5(LT_{RATE}) + \beta_6(LP_{RATE})$	0.41
19	$D_{PATHWISE}$	$\beta_0 + \beta_1(Time) + \beta_2(GT) + \beta_3(LT) + \beta_4(LP) + \beta_5(LT_{RATE}) + \beta_6(LP_{RATE})$	0.67
20	$D_{PATHWISE}$	$\beta_0 + \beta_1(Time) + \beta_2(GT) + \beta_3(LT) + \beta_4(LP) + \beta_5(LT_{RATE}) + \beta_6(LP_{RATE})$	0.64
21	$D_{PATHWISE}$	$\beta_0 + \beta_1(Time) + \beta_2(GT) + \beta_3(LT) + \beta_4(LP) + \beta_5(LT_{RATE}) + \beta_6(LP_{RATE})$	0.41
22	$D_{PATHWISE}$	$\beta_0 + \beta_1(Time) + \beta_2(GT) + \beta_3(LT) + \beta_4(LP) + \beta_5(LT_{RATE}) + \beta_6(LP_{RATE})$	0.55
23	$D_{PATHWISE}$	$\beta_0 + \beta_1(Time) + \beta_2(GT) + \beta_3(LT) + \beta_4(LP) + \beta_5(LT_{RATE}) + \beta_6(LP_{RATE})$	0.59
24	$D_{PATHWISE}$	$\beta_0 + \beta_1(Time) + \beta_2(GT) + \beta_3(LT) + \beta_4(LP) + \beta_5(LT_{RATE}) + \beta_6(LP_{RATE})$	0.57
25	$D_{PATHWISE}$	$\beta_0 + \beta_1(Time) + \beta_2(GT) + \beta_3(LT) + \beta_4(LP) + \beta_5(LT_{RATE}) + \beta_6(LP_{RATE})$	0.69
26	$D_{PATHWISE}$	$\beta_0 + \beta_1(Time) + \beta_2(GT) + \beta_3(LT) + \beta_4(LP) + \beta_5(LT_{RATE}) + \beta_6(LP_{RATE})$	0.63
27	$D_{PATHWISE}$	$\beta_0 + \beta_1(Time) + \beta_2(GT) + \beta_3(LT) + \beta_4(LP) + \beta_5(LT_{RATE}) + \beta_6(LP_{RATE})$	0.41
28	$D_{PATHWISE}$	$\beta_0 + \beta_1(Time) + \beta_2(GT) + \beta_3(LT) + \beta_4(LP) + \beta_5(LT_{RATE}) + \beta_6(LP_{RATE})$	0.47
29	$D_{PATHWISE}$	$\beta_0 + \beta_1(Time) + \beta_2(GT) + \beta_3(LT) + \beta_4(LP) + \beta_5(LT_{RATE}) + \beta_6(LP_{RATE})$	0.57
30	$D_{PATHWISE}$	$\beta_0 + \beta_1(Time) + \beta_2(GT) + \beta_3(LT) + \beta_4(LP) + \beta_5(LT_{RATE}) + \beta_6(LP_{RATE})$	0.54
31	$D_{PATHWISE}$	$\beta_0 + \beta_1(Time) + \beta_2(GT) + \beta_3(LT) + \beta_4(LP) + \beta_5(LT_{RATE}) + \beta_6(LP_{RATE})$	0.59
32	$D_{PATHWISE}$	$\beta_0 + \beta_1(Time) + \beta_2(GT) + \beta_3(LT) + \beta_4(LP) + \beta_5(LT_{RATE}) + \beta_6(LP_{RATE})$	0.62

33	$D_{PATHWISE}$	$\beta_0 + \beta_1(Time) + \beta_2(GT) + \beta_3(LT) + \beta_4(LP) + \beta_5(LT_{RATE}) + \beta_6(LP_{RATE})$	0.63
34	$D_{PATHWISE}$	$\beta_0 + \beta_1(Time) + \beta_2(GT) + \beta_3(LT) + \beta_4(LP) + \beta_5(LT_{RATE}) + \beta_6(LP_{RATE})$	0.55
35	$D_{PATHWISE}$	$\beta_0 + \beta_1(Time) + \beta_2(GT) + \beta_3(LT) + \beta_4(LP) + \beta_5(LT_{RATE}) + \beta_6(LP_{RATE})$	0.59
36	$D_{PATHWISE}$	$\beta_0 + \beta_1(Time) + \beta_2(GT) + \beta_3(LT) + \beta_4(LP) + \beta_5(LT_{RATE}) + \beta_6(LP_{RATE})$	0.59
37	$D_{PATHWISE}$	$\beta_0 + \beta_1(Time) + \beta_2(GT) + \beta_3(LT) + \beta_4(LP) + \beta_5(LT_{RATE}) + \beta_6(LP_{RATE})$	0.44
38	$D_{PATHWISE}$	$\beta_0 + \beta_1(Time) + \beta_2(GT) + \beta_3(LT) + \beta_4(LP) + \beta_5(LT_{RATE}) + \beta_6(LP_{RATE})$	0.60
39	$D_{PATHWISE}$	$\beta_0 + \beta_1(Time) + \beta_2(GT) + \beta_3(LT) + \beta_4(LP) + \beta_5(LT_{RATE}) + \beta_6(LP_{RATE})$	0.48
40	$D_{PATHWISE}$	$\beta_0 + \beta_1(Time) + \beta_2(GT) + \beta_3(LT) + \beta_4(LP) + \beta_5(LT_{RATE}) + \beta_6(LP_{RATE})$	0.51
41	$D_{PATHWISE}$	$\beta_0 + \beta_1(Time) + \beta_2(GT) + \beta_3(LT) + \beta_4(LP) + \beta_5(LT_{RATE}) + \beta_6(LP_{RATE})$	0.37
42	$D_{PATHWISE}$	$\beta_0 + \beta_1(Time) + \beta_2(GT) + \beta_3(LT) + \beta_4(LP) + \beta_5(LT_{RATE}) + \beta_6(LP_{RATE})$	0.51
43	$D_{PATHWISE}$	$\beta_0 + \beta_1(Time) + \beta_2(GT) + \beta_3(LT) + \beta_4(LP) + \beta_5(LT_{RATE}) + \beta_6(LP_{RATE})$	0.52
44	$D_{PATHWISE}$	$\beta_0 + \beta_1(Time) + \beta_2(GT) + \beta_3(LT) + \beta_4(LP) + \beta_5(LT_{RATE}) + \beta_6(LP_{RATE})$	0.64
45	$D_{PATHWISE}$	$\beta_0 + \beta_1(Time) + \beta_2(GT) + \beta_3(LT) + \beta_4(LP) + \beta_5(LT_{RATE}) + \beta_6(LP_{RATE})$	0.61
46	$D_{PATHWISE}$	$\beta_0 + \beta_1(Time) + \beta_2(GT) + \beta_3(LT) + \beta_4(LP) + \beta_5(LT_{RATE}) + \beta_6(LP_{RATE})$	0.45
47	$D_{PATHWISE}$	$\beta_0 + \beta_1(Time) + \beta_2(GT) + \beta_3(LT) + \beta_4(LP) + \beta_5(LT_{RATE}) + \beta_6(LP_{RATE})$	0.41
48	$D_{PATHWISE}$	$\beta_0 + \beta_1(Time) + \beta_2(GT) + \beta_3(LT) + \beta_4(LP) + \beta_5(LT_{RATE}) + \beta_6(LP_{RATE})$	0.57
49	$D_{PATHWISE}$	$\beta_0 + \beta_1(Time) + \beta_2(GT) + \beta_3(LT) + \beta_4(LP) + \beta_5(LT_{RATE}) + \beta_6(LP_{RATE})$	0.64
50	$D_{PATHWISE}$	$\beta_0 + \beta_1(Time) + \beta_2(GT) + \beta_3(LT) + \beta_4(LP) + \beta_5(LT_{RATE}) + \beta_6(LP_{RATE})$	0.42
51	$D_{PATHWISE}$	$\beta_0 + \beta_1(Time) + \beta_2(GT) + \beta_3(LT) + \beta_4(LP) + \beta_5(LT_{RATE}) + \beta_6(LP_{RATE})$	0.66
52	$D_{PATHWISE}$	$\beta_0 + \beta_1(Time) + \beta_2(GT) + \beta_3(LT) + \beta_4(LP) + \beta_5(LT_{RATE}) + \beta_6(LP_{RATE})$	0.47
53	$D_{PATHWISE}$	$\beta_0 + \beta_1(Time) + \beta_2(GT) + \beta_3(LT) + \beta_4(LP) + \beta_5(LT_{RATE}) + \beta_6(LP_{RATE})$	0.46
54	$D_{PATHWISE}$	$\beta_0 + \beta_1(Time) + \beta_2(GT) + \beta_3(LT) + \beta_4(LP) + \beta_5(LT_{RATE}) + \beta_6(LP_{RATE})$	0.45
55	$D_{PATHWISE}$	$\beta_0 + \beta_1(Time) + \beta_2(GT) + \beta_3(LT) + \beta_4(LP) + \beta_5(LT_{RATE}) + \beta_6(LP_{RATE})$	0.58
56	$D_{PATHWISE}$	$\beta_0 + \beta_1(Time) + \beta_2(GT) + \beta_3(LT) + \beta_4(LP) + \beta_5(LT_{RATE}) + \beta_6(LP_{RATE})$	0.61
57	$D_{PATHWISE}$	$\beta_0 + \beta_1(Time) + \beta_2(GT) + \beta_3(LT) + \beta_4(LP) + \beta_5(LT_{RATE}) + \beta_6(LP_{RATE})$	0.40
58	$D_{PATHWISE}$	$\beta_0 + \beta_1(Time) + \beta_2(GT) + \beta_3(LT) + \beta_4(LP) + \beta_5(LT_{RATE}) + \beta_6(LP_{RATE})$	0.57
59	$D_{PATHWISE}$	$\beta_0 + \beta_1(Time) + \beta_2(GT) + \beta_3(LT) + \beta_4(LP) + \beta_5(LT_{RATE}) + \beta_6(LP_{RATE})$	0.60
60	$D_{PATHWISE}$	$\beta_0 + \beta_1(Time) + \beta_2(GT) + \beta_3(LT) + \beta_4(LP) + \beta_5(LT_{RATE}) + \beta_6(LP_{RATE})$	0.51
61	$D_{PATHWISE}$	$\beta_0 + \beta_1(Time) + \beta_2(GT) + \beta_3(LT) + \beta_4(LP) + \beta_5(LT_{RATE}) + \beta_6(LP_{RATE})$	0.45
62	$D_{PATHWISE}$	$\beta_0 + \beta_1(Time) + \beta_2(GT) + \beta_3(LT) + \beta_4(LP) + \beta_5(LT_{RATE}) + \beta_6(LP_{RATE})$	0.58
63	$D_{PATHWISE}$	$\beta_0 + \beta_1(Time) + \beta_2(GT) + \beta_3(LT) + \beta_4(LP) + \beta_5(LT_{RATE}) + \beta_6(LP_{RATE})$	0.52
64	$D_{PATHWISE}$	$\beta_0 + \beta_1(Time) + \beta_2(GT) + \beta_3(LT) + \beta_4(LP) + \beta_5(LT_{RATE}) + \beta_6(LP_{RATE})$	0.60
65	$D_{PATHWISE}$	$\beta_0 + \beta_1(Time) + \beta_2(GT) + \beta_3(LT) + \beta_4(LP) + \beta_5(LT_{RATE}) + \beta_6(LP_{RATE})$	0.51
66	$D_{PATHWISE}$	$\beta_0 + \beta_1(Time) + \beta_2(GT) + \beta_3(LT) + \beta_4(LP) + \beta_5(LT_{RATE}) + \beta_6(LP_{RATE})$	0.59
67	$D_{PATHWISE}$	$\beta_0 + \beta_1(Time) + \beta_2(GT) + \beta_3(LT) + \beta_4(LP) + \beta_5(LT_{RATE}) + \beta_6(LP_{RATE})$	0.54
68	$D_{PATHWISE}$	$\beta_0 + \beta_1(Time) + \beta_2(GT) + \beta_3(LT) + \beta_4(LP) + \beta_5(LT_{RATE}) + \beta_6(LP_{RATE})$	0.43

69	$D_{PATHWISE}$	$\beta_0 + \beta_1(Time) + \beta_2(GT) + \beta_3(LT) + \beta_4(LP) + \beta_5(LT_{RATE}) + \beta_6(LP_{RATE})$	0.63
70	$D_{PATHWISE}$	$\beta_0 + \beta_1(Time) + \beta_2(GT) + \beta_3(LT) + \beta_4(LP) + \beta_5(LT_{RATE}) + \beta_6(LP_{RATE})$	0.59
71	$D_{PATHWISE}$	$\beta_0 + \beta_1(Time) + \beta_2(GT) + \beta_3(LT) + \beta_4(LP) + \beta_5(LT_{RATE}) + \beta_6(LP_{RATE})$	0.59
72	$D_{PATHWISE}$	$\beta_0 + \beta_1(Time) + \beta_2(GT) + \beta_3(LT) + \beta_4(LP) + \beta_5(LT_{RATE}) + \beta_6(LP_{RATE})$	0.54
73	$D_{PATHWISE}$	$\beta_0 + \beta_1(Time) + \beta_2(GT) + \beta_3(LT) + \beta_4(LP) + \beta_5(LT_{RATE}) + \beta_6(LP_{RATE})$	0.47
74	$D_{PATHWISE}$	$\beta_0 + \beta_1(Time) + \beta_2(GT) + \beta_3(LT) + \beta_4(LP) + \beta_5(LT_{RATE}) + \beta_6(LP_{RATE})$	0.60
75	$D_{PATHWISE}$	$\beta_0 + \beta_1(Time) + \beta_2(GT) + \beta_3(LT) + \beta_4(LP) + \beta_5(LT_{RATE}) + \beta_6(LP_{RATE})$	0.64
76	$D_{PATHWISE}$	$\beta_0 + \beta_1(Time) + \beta_2(GT) + \beta_3(LT) + \beta_4(LP) + \beta_5(LT_{RATE}) + \beta_6(LP_{RATE})$	0.64
77	$D_{PATHWISE}$	$\beta_0 + \beta_1(Time) + \beta_2(GT) + \beta_3(LT) + \beta_4(LP) + \beta_5(LT_{RATE}) + \beta_6(LP_{RATE})$	0.44
78	$D_{PATHWISE}$	$\beta_0 + \beta_1(Time) + \beta_2(GT) + \beta_3(LT) + \beta_4(LP) + \beta_5(LT_{RATE}) + \beta_6(LP_{RATE})$	0.49
79	$D_{PATHWISE}$	$\beta_0 + \beta_1(Time) + \beta_2(GT) + \beta_3(LT) + \beta_4(LP) + \beta_5(LT_{RATE}) + \beta_6(LP_{RATE})$	0.63
80	$D_{PATHWISE}$	$\beta_0 + \beta_1(Time) + \beta_2(GT) + \beta_3(LT) + \beta_4(LP) + \beta_5(LT_{RATE}) + \beta_6(LP_{RATE})$	0.52
81	$D_{PATHWISE}$	$\beta_0 + \beta_1(Time) + \beta_2(GT) + \beta_3(LT) + \beta_4(LP) + \beta_5(LT_{RATE}) + \beta_6(LP_{RATE})$	0.59
82	$D_{PATHWISE}$	$\beta_0 + \beta_1(Time) + \beta_2(GT) + \beta_3(LT) + \beta_4(LP) + \beta_5(LT_{RATE}) + \beta_6(LP_{RATE})$	0.50
83	$D_{PATHWISE}$	$\beta_0 + \beta_1(Time) + \beta_2(GT) + \beta_3(LT) + \beta_4(LP) + \beta_5(LT_{RATE}) + \beta_6(LP_{RATE})$	0.56
84	$D_{PATHWISE}$	$\beta_0 + \beta_1(Time) + \beta_2(GT) + \beta_3(LT) + \beta_4(LP) + \beta_5(LT_{RATE}) + \beta_6(LP_{RATE})$	0.57
85	$D_{PATHWISE}$	$\beta_0 + \beta_1(Time) + \beta_2(GT) + \beta_3(LT) + \beta_4(LP) + \beta_5(LT_{RATE}) + \beta_6(LP_{RATE})$	0.61
86	$D_{PATHWISE}$	$\beta_0 + \beta_1(Time) + \beta_2(GT) + \beta_3(LT) + \beta_4(LP) + \beta_5(LT_{RATE}) + \beta_6(LP_{RATE})$	0.63
87	$D_{PATHWISE}$	$\beta_0 + \beta_1(Time) + \beta_2(GT) + \beta_3(LT) + \beta_4(LP) + \beta_5(LT_{RATE}) + \beta_6(LP_{RATE})$	0.46
88	$D_{PATHWISE}$	$\beta_0 + \beta_1(Time) + \beta_2(GT) + \beta_3(LT) + \beta_4(LP) + \beta_5(LT_{RATE}) + \beta_6(LP_{RATE})$	0.46
89	$D_{PATHWISE}$	$\beta_0 + \beta_1(Time) + \beta_2(GT) + \beta_3(LT) + \beta_4(LP) + \beta_5(LT_{RATE}) + \beta_6(LP_{RATE})$	0.60
90	$D_{PATHWISE}$	$\beta_0 + \beta_1(Time) + \beta_2(GT) + \beta_3(LT) + \beta_4(LP) + \beta_5(LT_{RATE}) + \beta_6(LP_{RATE})$	0.63
91	$D_{PATHWISE}$	$\beta_0 + \beta_1(Time) + \beta_2(GT) + \beta_3(LT) + \beta_4(LP) + \beta_5(LT_{RATE}) + \beta_6(LP_{RATE})$	0.59
92	$D_{PATHWISE}$	$\beta_0 + \beta_1(Time) + \beta_2(GT) + \beta_3(LT) + \beta_4(LP) + \beta_5(LT_{RATE}) + \beta_6(LP_{RATE})$	0.63
93	$D_{PATHWISE}$	$\beta_0 + \beta_1(Time) + \beta_2(GT) + \beta_3(LT) + \beta_4(LP) + \beta_5(LT_{RATE}) + \beta_6(LP_{RATE})$	0.54
94	$D_{PATHWISE}$	$\beta_0 + \beta_1(Time) + \beta_2(GT) + \beta_3(LT) + \beta_4(LP) + \beta_5(LT_{RATE}) + \beta_6(LP_{RATE})$	0.60
95	$D_{PATHWISE}$	$\beta_0 + \beta_1(Time) + \beta_2(GT) + \beta_3(LT) + \beta_4(LP) + \beta_5(LT_{RATE}) + \beta_6(LP_{RATE})$	0.60
96	$D_{PATHWISE}$	$\beta_0 + \beta_1(Time) + \beta_2(GT) + \beta_3(LT) + \beta_4(LP) + \beta_5(LT_{RATE}) + \beta_6(LP_{RATE})$	0.58
97	$D_{PATHWISE}$	$\beta_0 + \beta_1(Time) + \beta_2(GT) + \beta_3(LT) + \beta_4(LP) + \beta_5(LT_{RATE}) + \beta_6(LP_{RATE})$	0.46
98	$D_{PATHWISE}$	$\beta_0 + \beta_1(Time) + \beta_2(GT) + \beta_3(LT) + \beta_4(LP) + \beta_5(LT_{RATE}) + \beta_6(LP_{RATE})$	0.61
99	$D_{PATHWISE}$	$\beta_0 + \beta_1(Time) + \beta_2(GT) + \beta_3(LT) + \beta_4(LP) + \beta_5(LT_{RATE}) + \beta_6(LP_{RATE})$	0.61
100	$D_{PATHWISE}$	$\beta_0 + \beta_1(Time) + \beta_2(GT) + \beta_3(LT) + \beta_4(LP) + \beta_5(LT_{RATE}) + \beta_6(LP_{RATE})$	0.65

Extended Data Table 7.
Phylogenetic regression predicting $NC_{PATHWISE}$ across the sample of 100 phylogenetic trees of Euprimates. $P_{MCMC} < 0.05$ indicates predictor statistically significant effect.

Sample Tree	P_{MCMC} Intercept	P_{MCMC} Time	P_{MCMC} GT	P_{MCMC} LT	P_{MCMC} LP	P_{MCMC} LT_{RATE}	P_{MCMC} LP_{RATE}	R^2
1	0.001	0.002	0.112	0.046	0.026	0.894	0.001	0.54
2	0.001	0.001	0.236	0.052	0.008	0.026	0.001	0.45
3	0.004	0.002	0.102	0.196	0.004	0.574	0.001	0.55
4	0.001	0.001	0.498	0.19	0.012	0.248	0.001	0.42
5	0.001	0.001	0.18	0.072	0.002	0.11	0.001	0.45
6	0.001	0.001	0.19	0.05	0.01	0.124	0.001	0.45
7	0.001	0.001	0.136	0.058	0.016	0.462	0.001	0.45
8	0.001	0.001	0.152	0.042	0.016	0.35	0.001	0.47
9	0.001	0.001	0.1	0.112	0.006	0.486	0.001	0.57
10	0.001	0.001	0.13	0.062	0.014	0.37	0.002	0.42
11	0.001	0.001	0.178	0.034	0.012	0.384	0.001	0.47
12	0.001	0.002	0.246	0.022	0.02	0.086	0.001	0.43
13	0.001	0.006	0.164	0.096	0.006	0.548	0.001	0.52
14	0.001	0.01	0.582	0.062	0.014	0.028	0.001	0.41
15	0.001	0.001	0.038	0.072	0.01	0.358	0.001	0.49
16	0.001	0.004	0.194	0.142	0.006	0.604	0.001	0.43
17	0.004	0.002	0.094	0.096	0.016	0.842	0.001	0.53
18	0.001	0.004	0.266	0.138	0.001	0.79	0.001	0.46
19	0.001	0.001	0.314	0.052	0.004	0.12	0.001	0.43
20	0.001	0.001	0.102	0.034	0.02	0.76	0.001	0.47
21	0.001	0.004	0.15	0.04	0.001	0.972	0.001	0.55
22	0.001	0.001	0.13	0.088	0.016	0.544	0.001	0.48
23	0.001	0.004	0.222	0.066	0.02	0.3	0.001	0.44
24	0.001	0.001	0.23	0.122	0.028	0.72	0.001	0.41
25	0.001	0.002	0.218	0.056	0.016	0.012	0.001	0.45
26	0.001	0.001	0.098	0.052	0.058	0.506	0.001	0.51
27	0.001	0.004	0.254	0.068	0.001	0.724	0.001	0.52
28	0.001	0.002	0.09	0.07	0.008	0.76	0.001	0.52
29	0.016	0.002	0.02	0.066	0.014	0.818	0.001	0.54
30	0.004	0.006	0.142	0.064	0.006	0.858	0.001	0.51
31	0.001	0.001	0.18	0.104	0.03	0.26	0.001	0.44
32	0.001	0.001	0.29	0.072	0.006	0.03	0.001	0.42

33	0.001	0.006	0.434	0.038	0.014	0.098	0.001	0.44
34	0.001	0.001	0.196	0.134	0.026	0.84	0.001	0.47
35	0.001	0.001	0.278	0.164	0.004	0.25	0.001	0.42
36	0.001	0.004	0.37	0.06	0.014	0.24	0.001	0.48
37	0.001	0.001	0.21	0.042	0.008	0.126	0.001	0.44
38	0.001	0.002	0.196	0.058	0.018	0.232	0.001	0.47
39	0.001	0.001	0.58	0.098	0.062	0.72	0.016	0.43
40	0.001	0.004	0.306	0.082	0.02	0.718	0.001	0.45
41	0.001	0.006	0.066	0.142	0.004	0.326	0.001	0.58
42	0.001	0.004	0.224	0.186	0.002	0.92	0.001	0.46
43	0.001	0.001	0.128	0.04	0.034	0.734	0.001	0.44
44	0.001	0.004	0.248	0.014	0.01	0.076	0.001	0.46
45	0.001	0.001	0.118	0.036	0.012	0.234	0.001	0.48
46	0.001	0.004	0.176	0.034	0.004	0.408	0.001	0.56
47	0.001	0.008	0.132	0.09	0.004	0.78	0.001	0.52
48	0.002	0.004	0.136	0.048	0.028	0.948	0.001	0.60
49	0.001	0.001	0.152	0.064	0.036	0.722	0.001	0.45
50	0.001	0.006	0.286	0.042	0.002	0.48	0.001	0.53
51	0.001	0.001	0.188	0.022	0.016	0.054	0.001	0.50
52	0.001	0.004	0.148	0.08	0.006	0.786	0.001	0.49
53	0.001	0.001	0.08	0.132	0.008	0.288	0.002	0.53
54	0.002	0.014	0.108	0.056	0.006	0.844	0.001	0.53
55	0.001	0.001	0.276	0.082	0.014	0.184	0.001	0.44
56	0.001	0.001	0.194	0.008	0.004	0.036	0.001	0.47
57	0.001	0.016	0.152	0.076	0.001	0.804	0.001	0.52
58	0.001	0.002	0.26	0.054	0.024	0.37	0.001	0.47
59	0.001	0.004	0.082	0.054	0.026	0.39	0.001	0.46
60	0.001	0.006	0.21	0.078	0.018	0.648	0.001	0.45
61	0.001	0.001	0.21	0.104	0.018	0.396	0.001	0.46
62	0.001	0.001	0.202	0.056	0.012	0.06	0.001	0.46
63	0.001	0.001	0.248	0.136	0.038	0.556	0.001	0.45
64	0.001	0.001	0.358	0.06	0.016	0.24	0.001	0.43
65	0.001	0.001	0.222	0.08	0.004	0.374	0.001	0.49
66	0.001	0.008	0.498	0.104	0.012	0.574	0.001	0.44
67	0.001	0.001	0.182	0.038	0.016	0.432	0.001	0.42
68	0.002	0.001	0.124	0.166	0.012	0.754	0.001	0.51

69	0.001	0.002	0.362	0.146	0.026	0.476	0.001	0.39
70	0.001	0.001	0.252	0.07	0.036	0.258	0.001	0.45
71	0.001	0.001	0.218	0.098	0.032	0.424	0.001	0.44
72	0.001	0.002	0.242	0.086	0.04	0.432	0.001	0.45
73	0.001	0.008	0.108	0.12	0.002	0.99	0.001	0.49
74	0.001	0.001	0.166	0.02	0.012	0.378	0.001	0.47
75	0.001	0.001	0.228	0.08	0.004	0.094	0.001	0.41
76	0.001	0.001	0.244	0.054	0.008	0.286	0.001	0.44
77	0.002	0.048	0.498	0.1	0.001	0.608	0.001	0.53
78	0.001	0.006	0.098	0.102	0.01	0.928	0.001	0.50
79	0.001	0.002	0.234	0.054	0.014	0.454	0.001	0.46
80	0.001	0.001	0.222	0.054	0.008	0.628	0.001	0.47
81	0.014	0.006	0.092	0.094	0.008	0.35	0.001	0.53
82	0.001	0.008	0.324	0.12	0.014	0.978	0.001	0.45
83	0.001	0.001	0.062	0.064	0.06	0.32	0.001	0.46
84	0.001	0.001	0.288	0.078	0.01	0.264	0.001	0.42
85	0.001	0.001	0.196	0.058	0.012	0.256	0.001	0.45
86	0.001	0.002	0.184	0.174	0.002	0.476	0.001	0.43
87	0.001	0.008	0.3	0.06	0.002	0.722	0.001	0.51
88	0.001	0.01	0.106	0.128	0.008	0.548	0.001	0.53
89	0.001	0.001	0.312	0.048	0.001	0.044	0.001	0.47
90	0.001	0.002	0.248	0.052	0.012	0.33	0.001	0.47
91	0.001	0.001	0.302	0.144	0.042	0.808	0.001	0.45
92	0.001	0.002	0.284	0.084	0.01	0.366	0.001	0.42
93	0.001	0.001	0.334	0.136	0.014	0.27	0.001	0.43
94	0.002	0.001	0.094	0.03	0.016	0.068	0.001	0.50
95	0.001	0.001	0.122	0.048	0.022	0.294	0.001	0.45
96	0.001	0.001	0.4	0.058	0.002	0.158	0.001	0.42
97	0.012	0.001	0.17	0.06	0.002	0.506	0.001	0.57
98	0.001	0.001	0.452	0.022	0.016	0.172	0.001	0.44
99	0.001	0.001	0.186	0.042	0.028	0.562	0.001	0.47
100	0.001	0.001	0.248	0.034	0.002	0.006	0.001	0.50